OAK RIDGE NATIONAL LABORATORY LIBRARIES
3 4456 0548390 0

ORNL-3616
UC-25 – Metals, Ceramics, and Materials
TID-4500 (29th ed.)

DIFFUSION OF TITANIUM-44 AND VANADIUM-48 IN TITANIUM

James F. Murdock

OAK RIDGE NATIONAL LABORATORY
CENTRAL RESEARCH LIBRARY
CIRCULATION SECTION
4500N ROOM 175
LIBRARY LOAN COPY
DO NOT TRANSFER TO ANOTHER PERSON.
if you wish someone else to see this report, send in name with report and the library will arrange a loan.
ORNL-118 (6-97)

OAK RIDGE NATIONAL LABORATORY
operated by
UNION CARBIDE CORPORATION
for the
U.S. ATOMIC ENERGY COMMISSION

LEGAL NOTICE

This report was prepared as an account of Government sponsored work. Neither the United States, nor the Commission, nor any person acting on behalf of the Commission:

A. Makes any warranty or representation, expressed or implied, with respect to the accuracy, completeness, or usefulness of the information contained in this report, or that the use of any information, apparatus, method, or process disclosed in this report may not infringe privately owned rights; or

B. Assumes any liabilities with respect to the use of, or for damages resulting from the use of any information, apparatus, method, or process disclosed in this report.

As used in the above, "person acting on behalf of the Commission" includes any employee or contractor of the Commission, or employee of such contractor, to the extent that such employee or contractor of the Commission, or employee of such contractor prepares, disseminates, or provides access to, any information pursuant to his employment or contract with the Commission, or his employment with such contractor.

ORNL-3616

Contract No. W-7405-eng-26

METALS AND CERAMICS DIVISION

DIFFUSION OF TITANIUM-44 AND VANADIUM-48 IN TITANIUM

James F. Murdock

JUNE 1964

OAK RIDGE NATIONAL LABORATORY
Oak Ridge, Tennessee
operated by
UNION CARBIDE CORPORATION
for the
U. S. ATOMIC ENERGY COMMISSION

OAK RIDGE NATIONAL LABORATORY LIBRARIES

3 4456 0548390 0

ACKNOWLEDGMENTS

The author wishes to thank Dr. E. E. Stansbury for his advice and encouragement throughout the graduate program.

The author was fortunate in having been able to perform the experimental work at the Oak Ridge National Laboratory; the assistance and advice of T. S. Lundy, J. I. Federer, J. H. Terry, R. A. Padgett, and T. L. Boswell of the Metals and Ceramics Division are gratefully acknowledged.

The drawings presented are the work of the Graphic Arts Department, Oak Ridge National Laboratory.

Special thanks are extended to F. R. Winslow of the Metals and Ceramics Division and to A. A. Brooks and Mrs. Kyleen Franz of the Oak Ridge Gaseous Diffusion Plant for their work in computer-fitting the experimental data. The advice and critical review of the mathematical content of this work by Dr. J. W. Prados, Chemical Engineering Department, University of Tennessee, proved invaluable.

The author also wishes to express his appreciation to the staff of the Metals and Ceramics Division Reports Office and especially Mrs. Frances Scarboro for the diligent attention given the preparation of this manuscript.

Thanks are extended to the Union Carbide Corporation, Nuclear Division, for its employee educational assistance program.

TABLE OF CONTENTS

CHAPTER		PAGE
I.	SUMMARY	1
II.	INTRODUCTION	3
III.	EXPERIMENTAL PROCEDURE	11
IV.	RESULTS	23
V.	DISCUSSION AND CONCLUSIONS	29
LIST OF REFERENCES		36
APPENDIX A.	Derivation of Fick's Second Law and Solution for Plane Source Semi-Infinite Geometry	41
APPENDIX B.	Secular Equilibrium	49
APPENDIX C.	Experimental Data and Sample Calculation	52
APPENDIX D.	FORTRAN Computer Program Used in Calculating Diffusion Coefficients	67

LIST OF TABLES

TABLE PAGE

I. Previous Experimental Data for Substitutional Diffusion in Titanium and Titanium Alloys 9

II. Major Impurity Levels in the Inactive Titanium 13

III. Diffusion Coefficients for Titanium-44 and Vanadium-48 in Titanium 27

IV. Experimental Data and Sample Calculation 52

LIST OF FIGURES

FIGURE PAGE

1. Geometry of the Diffusion Couple 12
2. Annealing Furnace for Use to 1150°C 16
3. Annealing Furnace for Use above 1150°C 17
4. Gamma Energy Spectrum of Titanium-44 from 0 to 2.5 Million Electron Volts 19
5. Gamma Energy Spectrum of Vanadium-48 from 0 to 2 Million Electron Volts 20
6. Penetration Profiles for the Diffusion of Titanium-44 in Titanium at 1200, 1337, and 1540°C 25
7. Penetration Profiles for the Diffusion of Vanadium-48 in Titanium at 1050, 1154, and 1370°C 26
8. Temperature Dependence of the Diffusion of Titanium-44 and Vanadium-48 in Titanium 28
9. Computer Fit of the Experimental Data for the Diffusion of Titanium-44 in Titanium to the Model Proposed by Kidson (55) 32
10. Computer Fit of the Experimental Data for the Diffusion of Vanadium-48 in Titanium to the Model Proposed by Kidson (55) 33
11. Temperature Dependence of the Apparent Activation Energy for the Diffusion of Titanium-44 and Vanadium-48 in Titanium and Zirconium-95 in Zirconium (55) 35
12. Differential Element of Volume 42

CHAPTER I

SUMMARY

The diffusion behavior of titanium-44 and vanadium-48 in body-centered cubic titanium was studied over the temperature range 900 to 1550°C using lathe sectioning and gamma spectrometry to determine the activity-distance profiles. Extensive use was made of the CDC 1604 and the IBM 7090 digital computers in analyzing the experimental data.

It was found that the Arrhenius-type equation, $D = D_o \exp\left(-\frac{Q}{RT}\right)$ with constant Q and D_o, did not adequately describe the temperature dependence of the diffusion coefficient. The data for both titanium-44 and vanadium-48 result in a plot of ln D versus 1/T which gives a continuously curving line over the entire temperature range. The apparent activation energies and frequency factors calculated from the slopes of those curves were found to increase with temperature. Computer-fitting the experimental ln D versus 1/T plot by the method of nonlinear least squares yielded the following equations which describe the behavior:

$$D_{Ti44} = 3.58 \times 10^{-4} \exp\left(-\frac{31,200}{RT}\right) + 1.09 \exp\left(-\frac{60,000}{RT}\right)$$

and

$$D_{V48} = 3.10 \times 10^{-4} \exp\left(-\frac{32,200}{RT}\right) + 1.37 \exp\left(-\frac{57,200}{RT}\right) .$$

Three possible explanations of the observed behavior are discussed: that the activation energy is a temperature-dependent function for a single mechanism; that diffusion along short-circuit paths predominates

at low temperatures; and that there may be two or more competing volume diffusion mechanisms. The proposed model of Kidson is seen to qualitatively explain the data. However, with the presently available data, no single explanation of the observed anomaly can as yet be ruled correct.

CHAPTER II

INTRODUCTION

"Wherefore no name can be found for a new fossil (element) which indicates its peculiar and characteristic properties, in which position I find myself at present, I think it is best to choose such a denomination as means nothing of itself and thus can give no rise to any erroneous ideas. In consequence of this, as I did in the case of uranium, I shall borrow the name for this metallic substance from mythology, and in particular from the Titans, the first sons of the earth. I therefore call this metallic genus, titanium (1)." Thus Martin Klaproth in 1795 named the element discovered by the Reverend William Gregor in 1790 — the element ninth in abundance in the lithosphere, the ten-mile-thick crust of the earth (1). The metallurgical impact of titanium has been great both as an alloy base and as an alloy addition. Barksdale (1) includes an excellent summary of some important metallurgical applications of titanium. Where lightweight strength was needed, in ordnance work, for example (2), titanium and titanium alloys have proved to be invaluable engineering materials.

In the basic understanding of the properties of metals and alloys and their useful applications, knowledge of the rate of mass transfer in the material is essential, particularly as the service temperature is raised. Chemical reaction, precipitation, and external corrosion, for example, all important to serviceability, may be controlled by the rate of mass transfer of some species in the material. The most common

method of studying mass transfer is to determine diffusion coefficients for the species of interest in the material.

Fundamentally, diffusion is the process by which a species moves from one part of a system to another through a series of random motions. Classically, diffusion is illustrated by partially filling a cylindrical column with a dye solution, then completely filling with water without mixing. The dye diffuses into the clear water progressively tinting lighter color toward the top. The works on diffusion would fill many volumes and are too numerous to list here, but an excellent history of diffusion was written by Seith and Heumann (3). In the books of Shewmon (4), Crank (5), and Jost (6), one finds the diffusion problem treated both theoretically and experimentally.

Fick first quantitatively developed the concept of a diffusion coefficient from an analogy to the heat conduction equations which Fourier (5) wrote. Fick arrived at two partial differential equations to describe the diffusion process. The first of these equations describes the flux through a plane in a direction normal to the plane, that is

$$F = -D\partial c/\partial x \tag{1}$$

where F is the rate of transfer per unit area of plane, c is the concentration of the diffusing species, x is the space coordinate normal to the plane, and D is the diffusion coefficient. The negative sign arises since the species diffuses in the direction of decreasing concentration. Rigorously, this equation applies only to diffusion in an isotropic

material. The second equation shows the variation of concentration with time, that is

$$\frac{\partial c}{\partial t} = \frac{D\partial^2 c}{\partial x^2} \tag{2}$$

where t is the time. The equation is derived for a concentration gradient in one direction. The second equation is derived from the first equation in Appendix A.

The most sensitive technique for studying diffusion is to follow the redistribution of a particular elemental species which is radioactive. Prewar (1945) experiments using the radioactive tracers were limited primarily to those species which occur radioactive in nature. The nuclear reactors and modern particle accelerators paved the way to an essentially unlimited supply of radioisotopes of virtually every element on the periodic table.

The most used radioactive tracer technique is to deposit a thin layer 50 to 100 Angstroms thick of the tracer species on one end of a right circular cylinder of the inactive material, anneal the specimen at an elevated temperature, and then determine the activity-distance profile of the tracer. Another technique is to locate all the tracer in a layer of known thickness, make a welded couple, anneal, and determine the activity-distance profile. The major difference in these techniques is the mathematical treatment of the activity-distance profile to yield a diffusion coefficient. Most variations of technique exist in the method of obtaining the activity-distance profile. Such variables as type of radioactive decay the tracer exhibits, the

half-life and specific activity of the tracer, the magnitude of the diffusion coefficient at the temperature of interest, and ductility of the inactive species determine the technique. The simplest method for determining the activity-distance profile is to mechanically remove thin layers of known thickness from the specimen normal to the direction of diffusion and determine the concentration of the tracer in each section. The thickness of each layer can be determined by a micrometer or by weighing the section and using the specimen density and diameter along with the weight to calculate the thickness. These mechanical sectioning methods include machining, lapping, microtome slicing, and hand grinding on polishing papers. In any method, determining the section thickness is the most important factor.

Early comprehensive tracer studies (7–37) concentrated on the face-centered cubic metals. Lazarus (38) presents a survey of these early works along with the present-day theories of atomic diffusion.

The basic conclusions of these investigators pertinent to this work are: (1) a linear variation of the logarithm of concentration of the diffusing species with the square of the penetration distance is found to represent lattice diffusion; (2) an Arrhenius-type equation represents the variation of the diffusion coefficient with temperature, that is

$$D = D_o \exp\left(-\frac{Q}{RT}\right) \tag{3}$$

where D is the diffusion coefficient in centimeters square per second, D_o is the frequency factor in centimeters square per second, Q is the activation energy in calories per mole, R is the gas constant in

calories per mole per degrees Kelvin, and T is the absolute temperature in degrees Kelvin; it has been found, in general, that D_o and Q are temperature independent within experimental errors; (3) theoretical considerations of mechanisms for diffusion in the face-centered cubic metals have led to the conclusion that the diffusion via lattice vacancies is the predominant mechanism for lattice diffusion in these metals. One would expect the frequency factor, D_o, to be in the order of one and the activation energy, Q, to be in the order of 32 T_m, where T_m is the absolute melting temperature from these theoretical considerations and from experimental results.

In recent years diffusion investigators (39–55) have turned their attention to the body-centered cubic metals. Lattice diffusion in the body-centered cubic metals has showed two trends as is pointed out by Peart et al. (47). There seem to be two distinct groups of body-centered cubic metals – the first group, alpha iron, niobium, molybdenum, and tantalum, which behave in a manner one would predict from the close-packed metals; the second group, beta titanium, beta zirconium, gamma uranium, and chromium, which behave very differently. The second group is characterized by frequency factors in the range 10^{-6} to 10^{-4} centimeters square per second and activation energies in the order of one third what one would expect from the melting point of the metals. Federer and Lundy (48) observed in the diffusion of niobium and zirconium in zirconium that the Arrhenius equation was not applicable over the temperature interval studied. Graham (49) reports similar behavior for solute diffusion in beta titanium over a wide temperature interval.

Both investigations (48, 49) revealed that plots of ln D versus 1/T were best fit by curved lines over the entire temperature range.

Inert marker movements have been observed in the titanium-molybdenum system in the temperature range 1400 to 1640°C, indicating a vacancy mechanism for diffusion in the titanium-molybdenum system and by implication all body-centered cubic transition metal systems (51). Similar inert marker movements have been observed in the titanium-vanadium (52), iron-chromium (53), and titanium-chromium (54) systems.

Kidson (55) has proposed that oxygen impurity enhancement of diffusion at low temperature may account for the deviations from linearity observed in the self-diffusion of zirconium. This idea will be pursued in more detail in the discussion with respect to titanium diffusion.

All the varied studies leave the theory of body-centered cubic diffusion very much in the realm of speculation at present. This work was undertaken to investigate the body-centered cubic diffusion problem further. The primary objective was to investigate diffusion in titanium over a wide temperature range in the body-centered cubic phase, particularly looking for the nonlinear Arrhenius behavior reported by Federer and Lundy (48) and Graham (49).

Previous experimental results for diffusion of substitutional elements in body-centered cubic titanium are given in Table I. These data are characterized by frequency factors ranging from 10^{-7} to 50 centimeters square per second and activation energies ranging from 30 to 60 kilocalories per mole. By comparing data in one system below

TABLE I

PREVIOUS EXPERIMENTAL DATA FOR SUBSTITUTIONAL DIFFUSION IN TITANIUM AND TITANIUM ALLOYS

Diffusing element	Alloy composition	Temperature range (°C)	Frequency factor, D_o (cm^2/sec)	Activation energy, Q (cal/mole)	Reference
Al	Ti–2 at. % Al	983–1250	1.4×10^{-5}	21,900	(52)
Al	Ti–12 at. % Al	983–1250	9.0×10^{-5}	25,500	(52)
Co^{60}	Ti	900–1250	1.2×10^{-2}	30,600	(49)
Co^{60}	Ti	1400–1650	1.1×10^{-1}	37,100	(49)
Cr^{51}	Ti(commercial)	980–1178	5.0×10^{-3}	35,300	(41)
Cr^{51}	Ti(iodide)	926–1193	1.0×10^{-2}	37,700	(41)
Cr^{51}	Ti–10 wt % Cr	926–1177	2.0×10^{-2}	40,200	(41)
Cr^{51}	Ti–18 wt % Cr	926–1178	9.0×10^{-2}	44,500	(41)
Fe^{55}	Ti(iodide)	900–1250	7.8×10^{-3}	31,600	(46)
Fe^{55}	Ti–5 at. % Fe	900–1250	9.2×10^{-2}	39,600	(46)
Fe^{55}	Ti–10 at. % Fe	900–1250	2.14	48,600	(46)
Fe^{55}	Ti–15 at. % Fe	900–1250	52.5	58,100	(46)
Fe^{55}	Ti–5 at. % Nb	900–1250	7.9×10^{-3}	33,100	(46)
Fe^{55}	Ti–10 at. % Nb	900–1250	11.5×10^{-3}	34,900	(46)
Fe^{55}	Ti–15 at. % Nb	900–1250	7.9×10^{-3}	35,000	(46)
Fe^{59}	Ti(iodide)	900–1250	8.5×10^{-3}	32,000	(46)
Fe^{59}	Ti(commercial)	900–1250	12.3×10^{-3}	32,900	(46)
Nb^{95}	Ti(commercial)	900–1250	5.0×10^{-3}	39,300	(46)
Nb^{95}	Ti–5 at. % Nb	900–1250	1.2×10^{-4}	29,900	(46)
Nb^{95}	Ti–10 at. % Nb	900–1250	5.8×10^{-4}	36,100	(46)
Nb^{95}	Ti–15 at. % Nb	900–1250	1.5×10^{-3}	39,300	(46)
Nb^{95}	Ti–5 at. % Fe	900–1250	1.82×10^{-9}	34,900	(46)
Nb^{95}	Ti–10 at. % Fe	900–1250	2.9×10^{-2}	41,300	(46)
Nb^{95}	Ti–15 at. % Fe	900–1250	9.9	56,000	(46)
Mn	Ti–8 at. % Mn	830–1190	1.0×10^{-3}	35,200	(52)
Mn^{54}	Ti(commercial)	900–1250	6.1×10^{-3}	33,700	(46)
Mn^{54}	Ti(commercial)	1400–1650	5.9×10^{-2}	39,600	(49)
Mo	Ti–1 at. % Mo	938–1248	1.0×10^{-5}	24,000	(52)
Mo^{99}	Ti(commercial)	900–1250	8.0×10^{-3}	43,000	(49)
Mo^{99}	Ti(commercial)	1400–1650	4.0×10^{-2}	47,000	(49)
Sn	Ti–1 at. % Sn	1004–1250	8.4×10^{-7}	15,300	(52)
Sn	Ti–8 at. % Sn	1090–1250	2.7×10^{-4}	29,800	(52)
Ni^{63}	Ti(commercial)	900–1250	9.2×10^{-3}	29,600	(46)
Ni^{63}	Ti(commercial)	1400–1650	2.9×10^{-1}	38,200	(49)

1200°C to data in the same system above 1400°C, one finds a variation of one and one-half times in the activation energy and a factor of as much as 200 in the frequency factor. These are consistent variations and well outside the normal range of experimental error.

CHAPTER III

EXPERIMENTAL PROCEDURE

The inactive titanium used in this work was 99.9 per cent titanium produced by the Foote Mineral Company using the iodide process. The as-received titanium was arc-melted into buttons three inches in diameter and five-eighths-inch thick on a water-cooled copper hearth in a tungsten electrode arc furnace. From these buttons, specimens five-eighths-inch diameter and one-half-inch long with a one-half-inch shank were machined as shown in Figure 1. The machined specimens were vacuum annealed at 1000°C for two days to lower the hydrogen content. After the vacuum anneal, the specimens were annealed at 1550°C for thirty minutes in fifteen pounds per square inch, gage, argon atmosphere to produce a stable beta grain size. The argon was used to prevent excessive thermal etching of the specimens. The resulting beta grains were equiaxed one-fourth- to three-eighths-inch diameter which remained stable during subsequent annealing. The chemical analysis of the titanium after these anneals is given in Table II. The large circular face of each specimen was polished metallographically through 3/0 emery paper and etched in a three-to-one solution of concentrated HNO_3 and HF, followed by a light polish on 3/0 paper and an etch to remove the worked surface.

The titanium-44 was produced in the 86-Inch Oak Ridge National Laboratory Cyclotron by the scandium-45 (p,2n) titanium-44 reactions. Carrier-free chemical separation of the titanium-44 from the scandium

UNCLASSIFIED
ORNL-DWG 63-8093

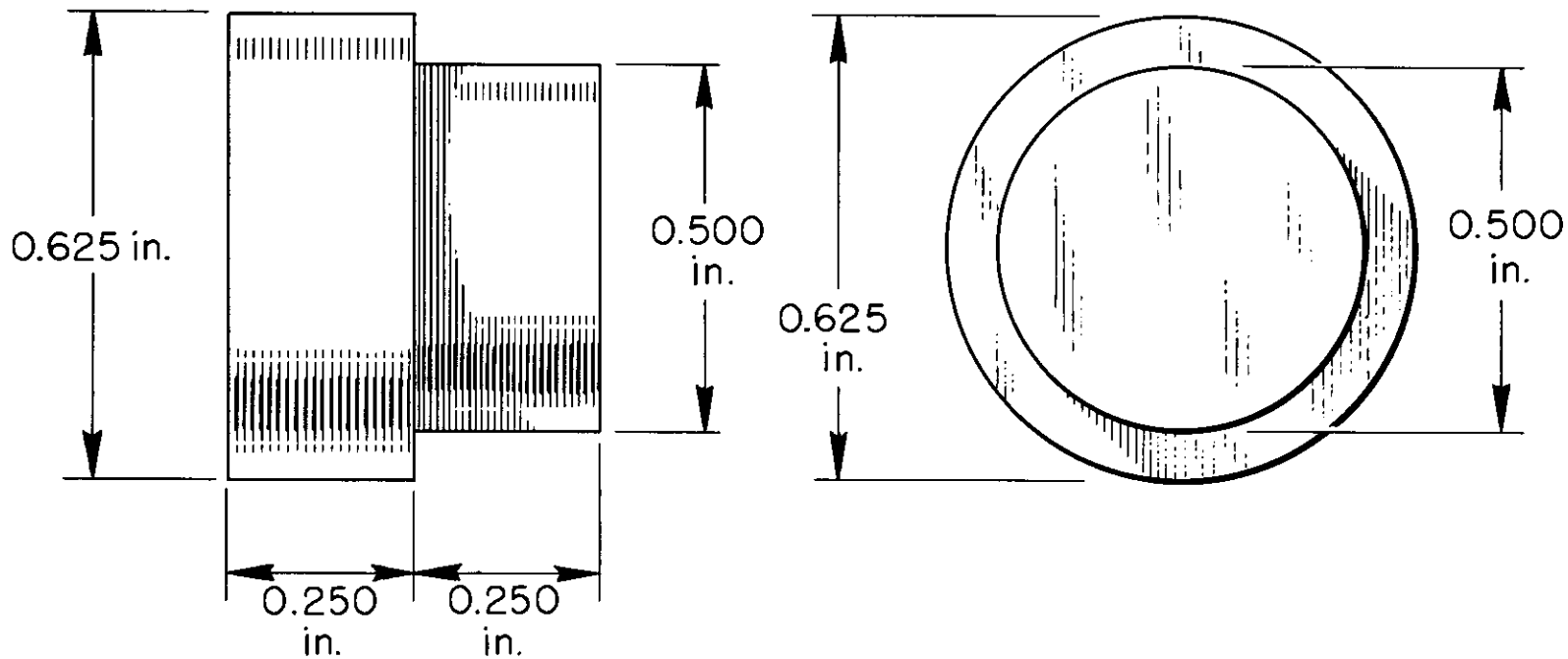

Figure 1. Geometry of the Diffusion Couple.

TABLE II

MAJOR IMPURITY LEVELS IN THE INACTIVE TITANIUM

Element	Concentration (ppm)
Cu	< 10
Mg	< 100
Mn	< 100
Si	100
H	6
O	120
N	100

target was performed by Nuclear Science and Engineering Corporation. Approximately three microcuries of titanium-44 were received in three milliliters of concentrated HCl.

The vanadium-48 was also produced in the 86-Inch Oak Ridge National Laboratory Cyclotron by the titanium-48 (p,n) vanadium-48. Other vanadium isotopes which could be produced from natural titanium by proton irradiation either have very short half-lives or have energies or modes of decay which do not conflict with vanadium-48. Carrier-free chemical separation of the vanadium-48 from the TiO_2 target was performed by the Oak Ridge National Laboratory Isotopes Division. Approximately two millicuries of vanadium-48 were received in ten milliliters of concentrated HNO_3.

The radioisotopes were deposited on the previously described polished faces of the inactive titanium by using micropipettes. The specific activity of the solutions determined the amount of each isotope necessary to perform the experiments. For the titanium-44-titanium experiments, 45 λ (1 $\lambda = 10^{-6}$ liters) of the as-received titanium-44 solution was deposited on each of the inactive titanium specimens and the solution was neutralized with NH_4OH which precipitated the titanium-44. The solution was then evaporated to dryness by means of a heat lamp, leaving a residue of NH_4Cl and hydrated $Ti^{44}O_2$. The NH_4Cl was evaporated and the TiO_2 was dried by sintering the specimens in an inert atmosphere at 500°C. For the vanadium-48-titanium experiments, 15 λ of the as-received vanadium-48 solution was deposited on each of the inactive

titanium specimens and the solution was evaporated to dryness by means of a heat lamp, leaving a residue of $HV^{48}O_3$.

Calculations showed that the thickness of the radioisotope layer was in the order of one atomic layer of titanium-44 and vanadium-48 so that any contamination from the oxygen in the layer from TiO_2 and HVO_3 was extremely low ($<<$ 1 ppm).

For diffusion anneals at 1150°C and below, the specimens were wrapped with 0.004-inch-thick titanium foil and encapsulated in quartz ampoules under 0.2-atmosphere absolute pressure of high-purity argon. The foil protected the specimens from chemical reaction with the quartz; the argon minimized specimen surface evaporation. The quartz ampoules containing the specimens were then placed in horizontal tube furnaces (Figure 2) which had been preheated to chosen temperatures. The temperatures were controlled by Wheelco Model-402 Capacitrol time-proportioning controllers. The sensing elements for the controllers were platinum versus platinum—10 per cent rhodium thermocouples placed against the inner wall of the furnace. The temperatures were measured using platinum versus platinum—10 per cent rhodium thermocouples which had been compared to a standard platinum versus platinum—10 per cent rhodium thermocouple calibrated at the melting points of gold, silver, aluminum, and zinc.

Diffusion anneals at temperatures above 1150°C were performed in furnaces having split-tube resistance-heating elements of tantalum (Figure 3). The temperatures were controlled by manually regulating the power input to the furnaces. The temperatures were measured using

UNCLASSIFIED
ORNL-DWG 63-8094

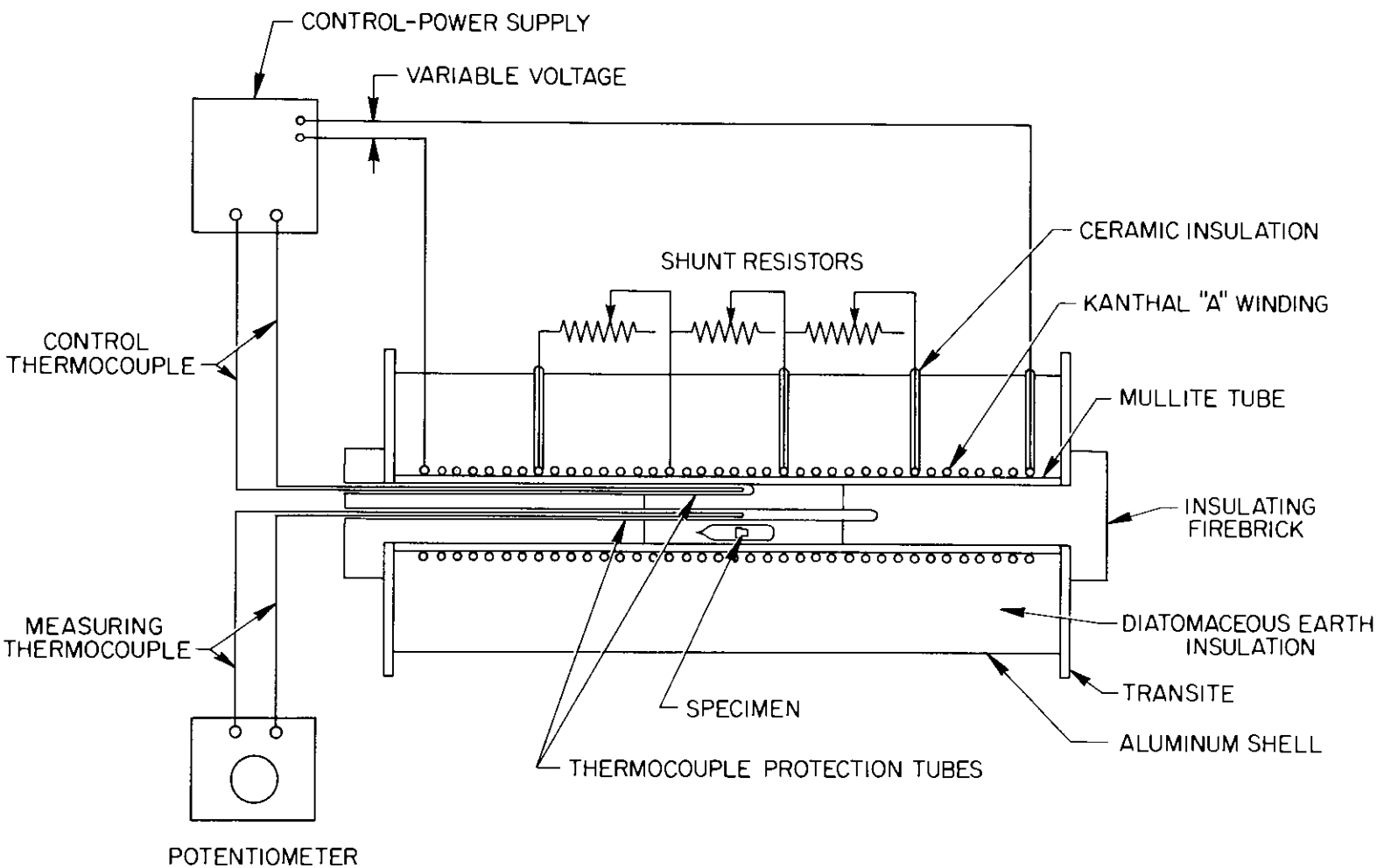

Figure 2. Annealing Furnace for Use to 1150°C.

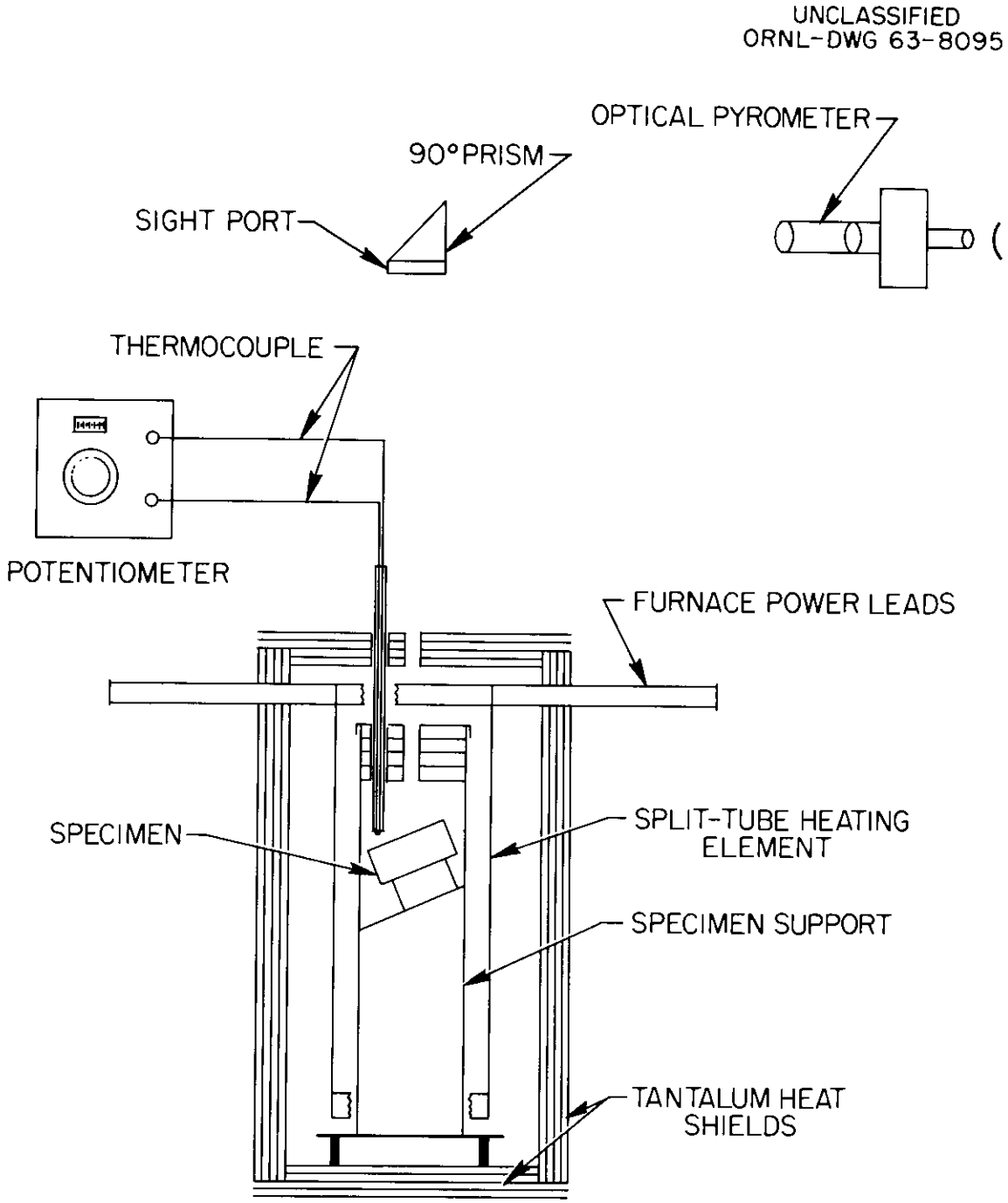

Figure 3. Annealing Furnace for Use above 1150°C.

a Pyro micro-optical pyrometer and by a platinum versus platinum-10 per cent rhodium thermocouple placed very near the surface of the specimens. The indicated control temperatures below 1150°C were ±0.5°C and the measured temperatures including a liberal allowance for calibration were ±2°C. The temperatures above 1150°C were estimated to vary from ±3°C at 1200°C to ±8°C at 1550°C.

After the diffusion anneals, each specimen was aligned in a lathe collet with the flat surface normal to the lathe axis and the five-eighths-inch diameter was reduced to approximately 0.550 inch to remove possible effects of surface diffusion. Sections 0.002-inch thick were machined from the specimens parallel to the flat surface to determine the activity-distance profiles. The sections were collected and weighed on a semimicrobalance. After weighing, the sections were individually taped to thin paper cards giving a geometry necessary for quantitatively determining the section activities. The activities were determined with a single-channel gamma spectrometer utilizing a three- by three-inch NaI (Tl) scintillation crystal as a detector.

The gamma energy spectra of the titanium-44 and vanadium-48 solutions are given in Figures 4 and 5. The titanium-44 decays by orbital-electron capture with a half-life of 10^3 years to scandium-44 which in turn decays by 94 per cent positron and 6 per cent orbital-electron capture with a half-life of 3.96 hours to stable calcium-44. Gamma energies of 0.070 and 0.074 million electron volts are associated with the decay of titanium-44 to scandium-44; gamma energies of 1.16 and a very weak 2.5 million electron volts are associated with the decay

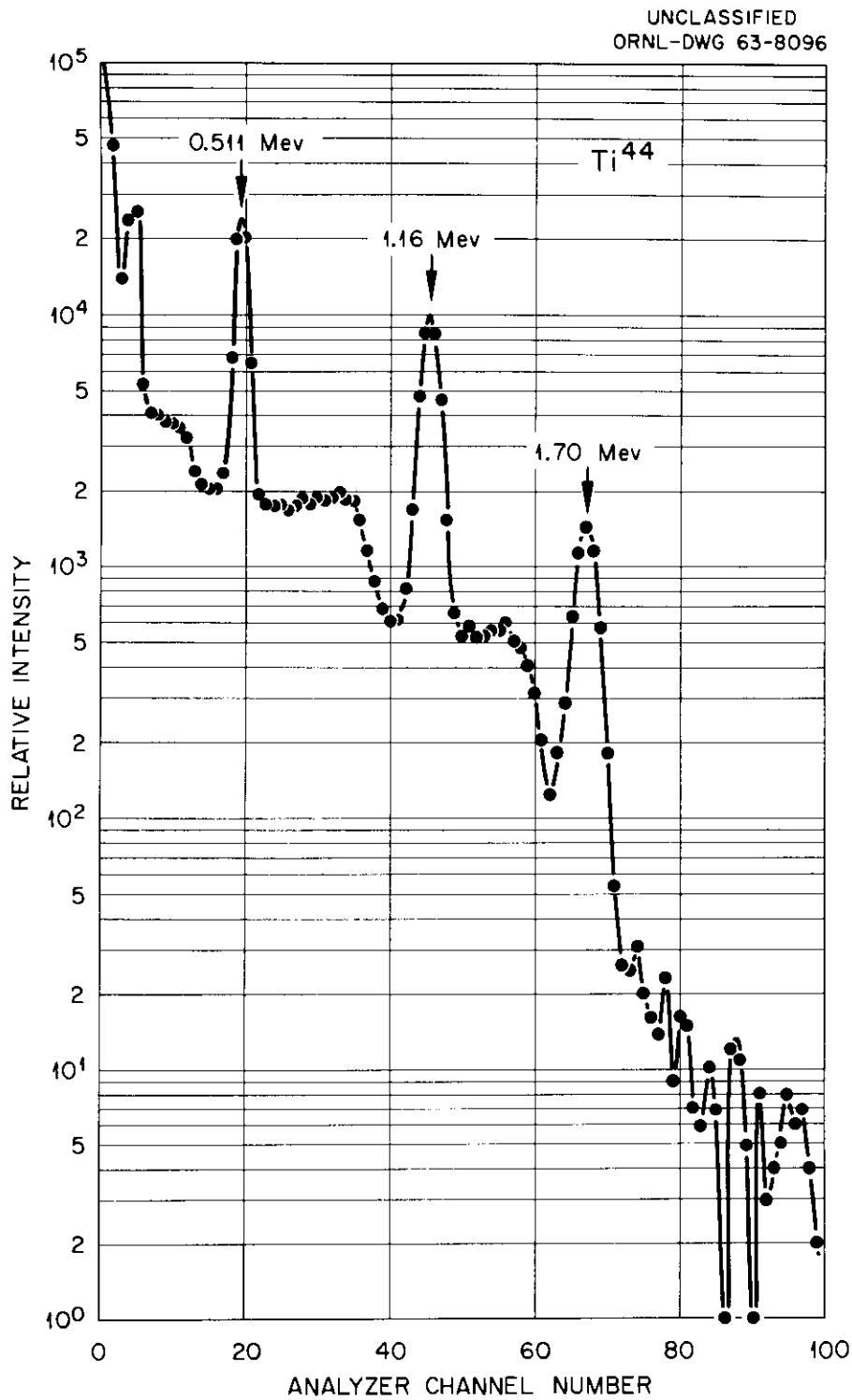

Figure 4. Gamma Energy Spectrum of Titanium-44 from 0 to 2.5 Million Electron Volts.

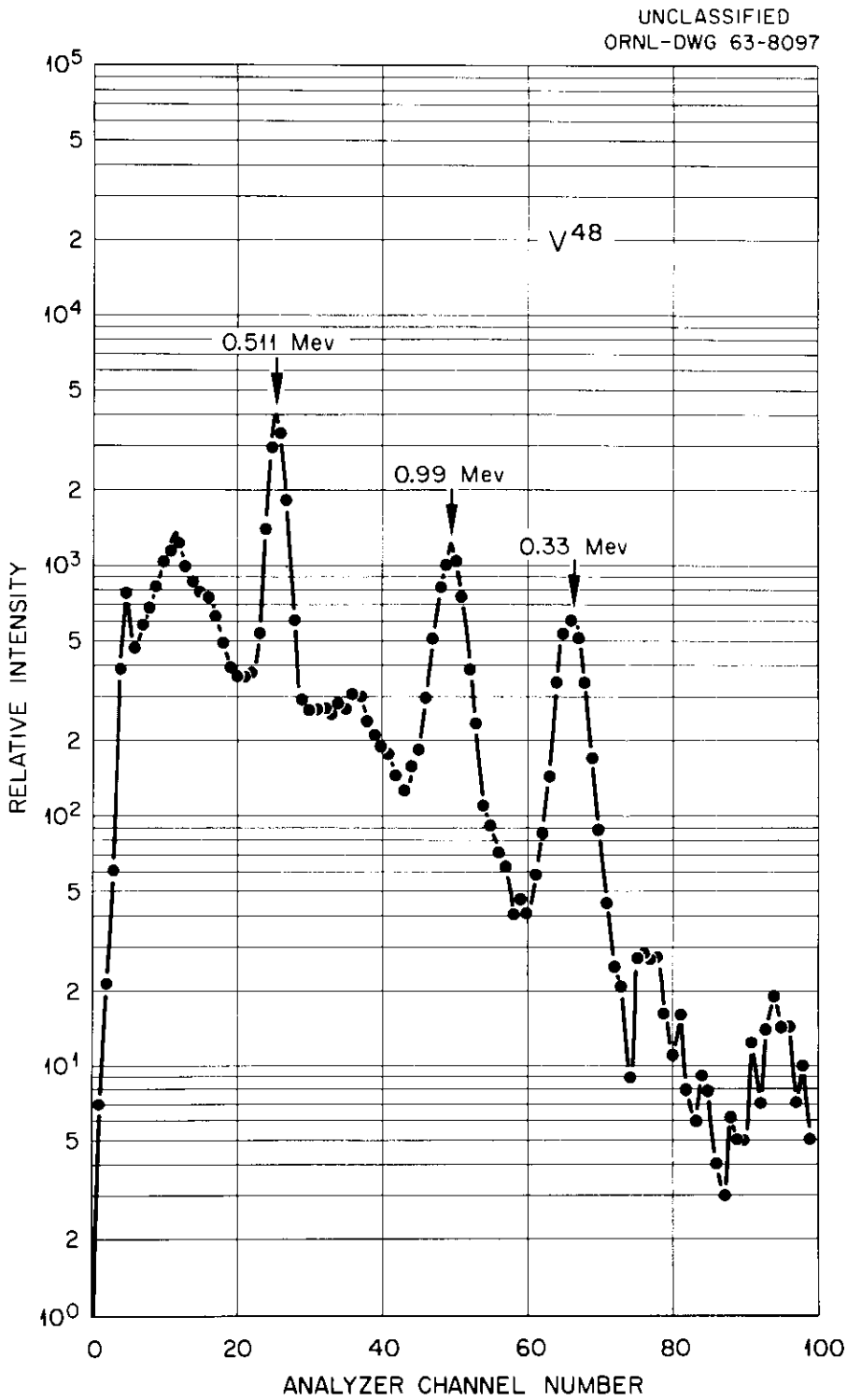

Figure 5. Gamma Energy Spectrum of Vanadium-48 from 0 to 2 Million Electron Volts.

of scandium-44 to calcium-44 (56). The titanium gamma energies were too low for easy accurate determinations, but the scandium-44 activity is proportional to the titanium-44 activity after secular equilibrium is reached. The concept of secular equilibrium is developed in Appendix B. The 1.16 million electron volts gamma of the scandium-44 was of sufficient intensity to allow the determination of the scandium-44 activity.

The contribution of the scandium-44 which diffused as scandium-44 to the specific activity of the section also was considered since one would expect scandium-44 to diffuse at a different rate than titanium-44. In order that this contribution be negligible, sufficient time was allowed after the diffusion anneal for "all" the scandium-44 formed during the anneal to decay.

In one half-life, 50 per cent of the original amount of activity decays; in two half-lives, 75 per cent of the original activity decays. So that after n half-lives, $100\left(1 - \frac{1}{2^n}\right)$ per cent of original activity will decay or $\frac{100}{2^n}$ per cent of the original activity remains. After four days, 5.34 times 10^{-6} per cent of the original scandium-44 will remain. A minimum of four days elapsed between the termination of the diffusion anneals and the scandium-44 activity determinations to allow the scandium-44 which diffused as scandium-44 to decay and for secular equilibrium to be reached between the diffused titanium-44 and scandium-44 product.

The vanadium-48 decays 57 per cent by positron and 43 per cent by orbital-electron capture with a half-life of 16.1 days to stable titanium-48. Gamma energies of 0.99, 1.33, and 2.22 million electron

volts are associated with this decay (56). The scandium-44 (titanium-44) activity was determined between 1.04 and 1.36 million electron volts which spanned the 1.16 million electron volts gamma peak. The vanadium-48 activity was determined between 0.86 and 1.10 million electron volts which spanned the 0.99 million electron volts gamma peak.

CHAPTER IV

RESULTS

The experimental data are: the weighing, activity, and counting time for each section; the annealing time and temperature; the thermal expansion from room temperature to the annealing temperature; and the specimen diameter. These data along with a complete sample calculation of a diffusion coefficient from the experimental data are included in Appendix C. The mathematical treatment of these data is discussed in this chapter.

The solution to Fick's second law applicable to the experimental conditions of this experiment is

$$c(x,t) = \frac{M}{\sqrt{\pi D t}} \exp\left(-\frac{x^2}{4Dt}\right) \tag{4}$$

where

$c(x,t)$ = the concentration of the diffusing species at some distance x from the original source after the annealing time t

M = the amount of diffusing species per unit area deposited at $x = 0$ and $t = 0$

D = the diffusion coefficient.

This solution is derived from Fick's second law in Appendix A. Examination of this equation reveals that a plot of $\ln c(x,t)$ versus x^2 should be linear with the slope inversely proportional to the diffusion coefficient. A measure of $c(x,t)$ for a diffusing radioactive species is the

specific activity of the species A(x,t). Since the slope of the concentration-distance plot is the parameter of interest, the value of $M/\sqrt{\pi Dt}$ need not be determined and only the relative specific activity of two succeeding sections is important. A FORTRAN computer program for the Control Data 1604 Digital Computer written by Winslow (57) was used in the calculation from the experimental data in Appendix C. This program is given in Appendix D. By the program instructions, the machine calculates the specific activity and the penetration distance squared, plots the logarithm specific activity versus x^2 using the Calcomp Plotter, determines and draws the best least squares fit of the data, calculates the diffusion coefficient, and calculates the 90 per cent confidence level deviation of the data from the least squares line.

Figures 6 and 7 are typical penetration profiles for titanium-44 and vanadium-48 diffusing into titanium. The diffusion coefficients are listed in Table III together with the annealing temperatures and the 90 per cent confidence level deviations. Arrhenius-type plots of ln D versus 1/T for titanium-44 and vanadium-48 are shown in Figure 8.

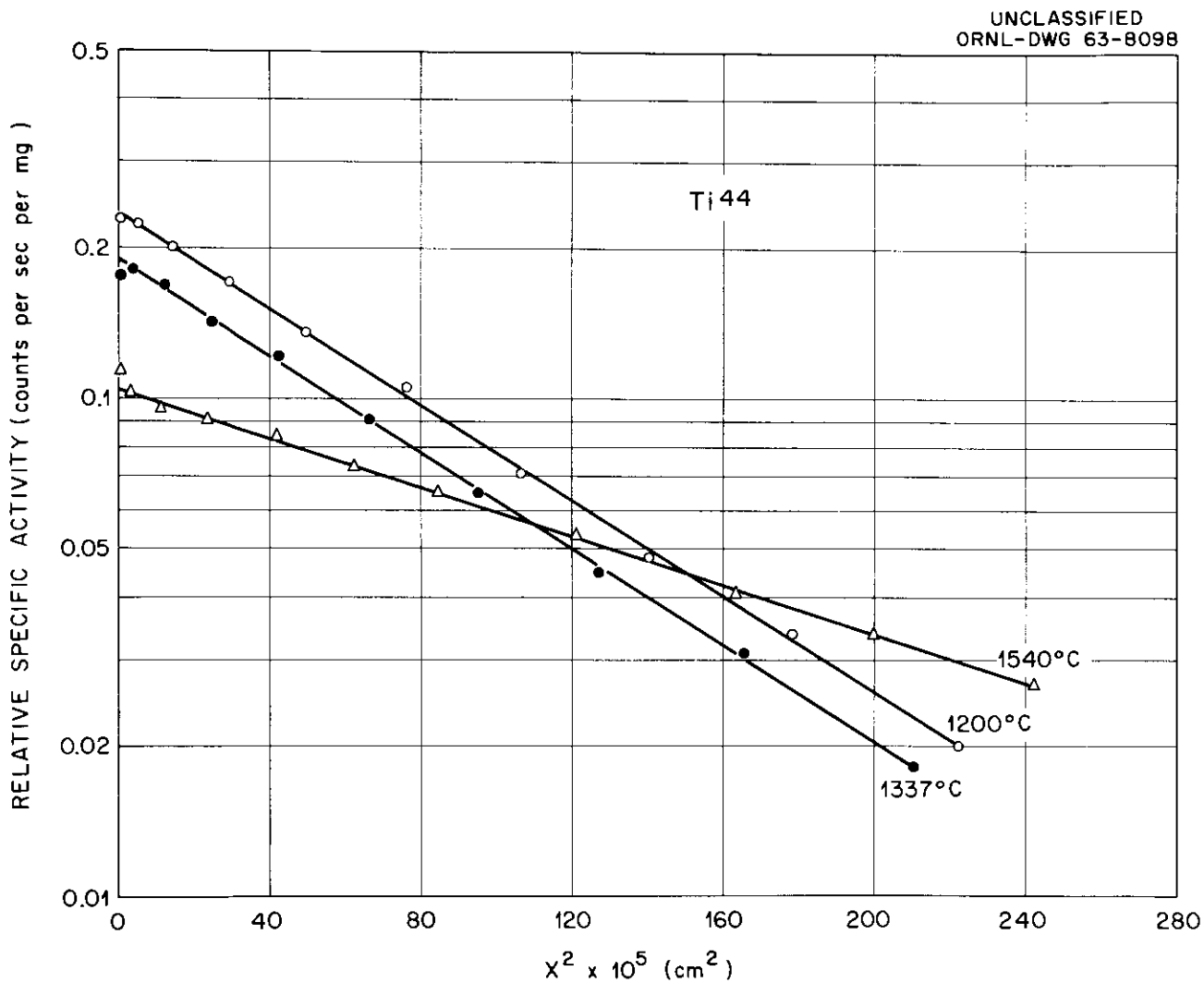

Figure 6. Penetration Profiles for the Diffusion of Titanium-44 in Titanium at 1200, 1337, and 1540°C.

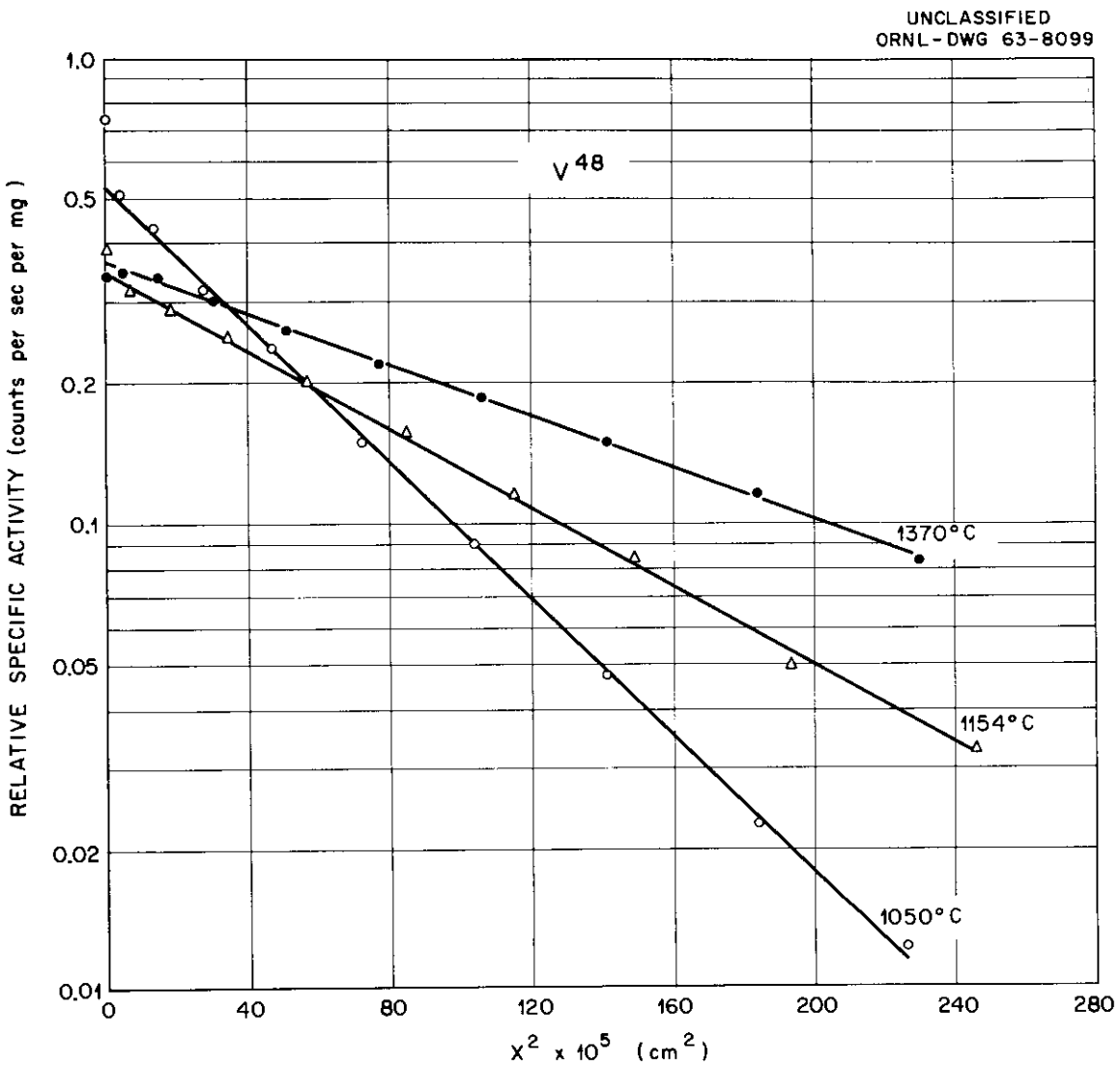

Figure 7. Penetration Profiles for the Diffusion of Vanadium-48 in Titanium at 1050, 1154, and 1370°C.

TABLE III

DIFFUSION COEFFICIENTS FOR TITANIUM-44 AND VANADIUM-48 IN TITANIUM

Titanium-44		Vanadium-48	
Temperature (°C)	D (cm^2/sec)	Temperature (°C)	D (cm^2/sec)
898.9	$(5.75 \pm 0.06) \times 10^{-10}$	901.5	$(3.63 \pm 0.07) \times 10^{-10}$
960	$(1.07 \pm 0.02) \times 10^{-9}$	952	$(6.58 \pm 0.07) \times 10^{-10}$
996.9	$(1.54 \pm 0.03) \times 10^{-9}$	999.5	$(1.16 \pm 0.03) \times 10^{-9}$
1053	$(2.86 \pm 0.09) \times 10^{-9}$	1050	$(2.05 \pm 0.04) \times 10^{-9}$
1093.5	$(3.71 \pm 0.16) \times 10^{-9}$	1099	$(3.43 \pm 0.04) \times 10^{-9}$
1148	$(6.45 \pm 0.27) \times 10^{-9}$	1154	$(5.97 \pm 0.17) \times 10^{-9}$
1200	$(9.56 \pm 0.16) \times 10^{-9}$	1200	$(9.66 \pm 0.10) \times 10^{-9}$
1249	$(1.34 \pm 0.03) \times 10^{-8}$	1250	$(1.87 \pm 0.03) \times 10^{-8}$
1300	$(2.04 \pm 0.03) \times 10^{-8}$	1308	$(3.27 \pm 0.05) \times 10^{-8}$
1337	$(3.10 \pm 0.05) \times 10^{-8}$	1370	$(5.03 \pm 0.11) \times 10^{-8}$
1385	$(3.85 \pm 0.06) \times 10^{-8}$	1450	$(1.02 \pm 0.02) \times 10^{-7}$
1450	$(6.56 \pm 0.06) \times 10^{-8}$	1500	$(1.52 \pm 0.04) \times 10^{-7}$
1489	$1.00 \pm 0.02 \times 10^{-7}$	1543	$(2.21 \pm 0.06) \times 10^{-7}$
1540	$(1.23 \pm 0.02) \times 10^{-7}$		

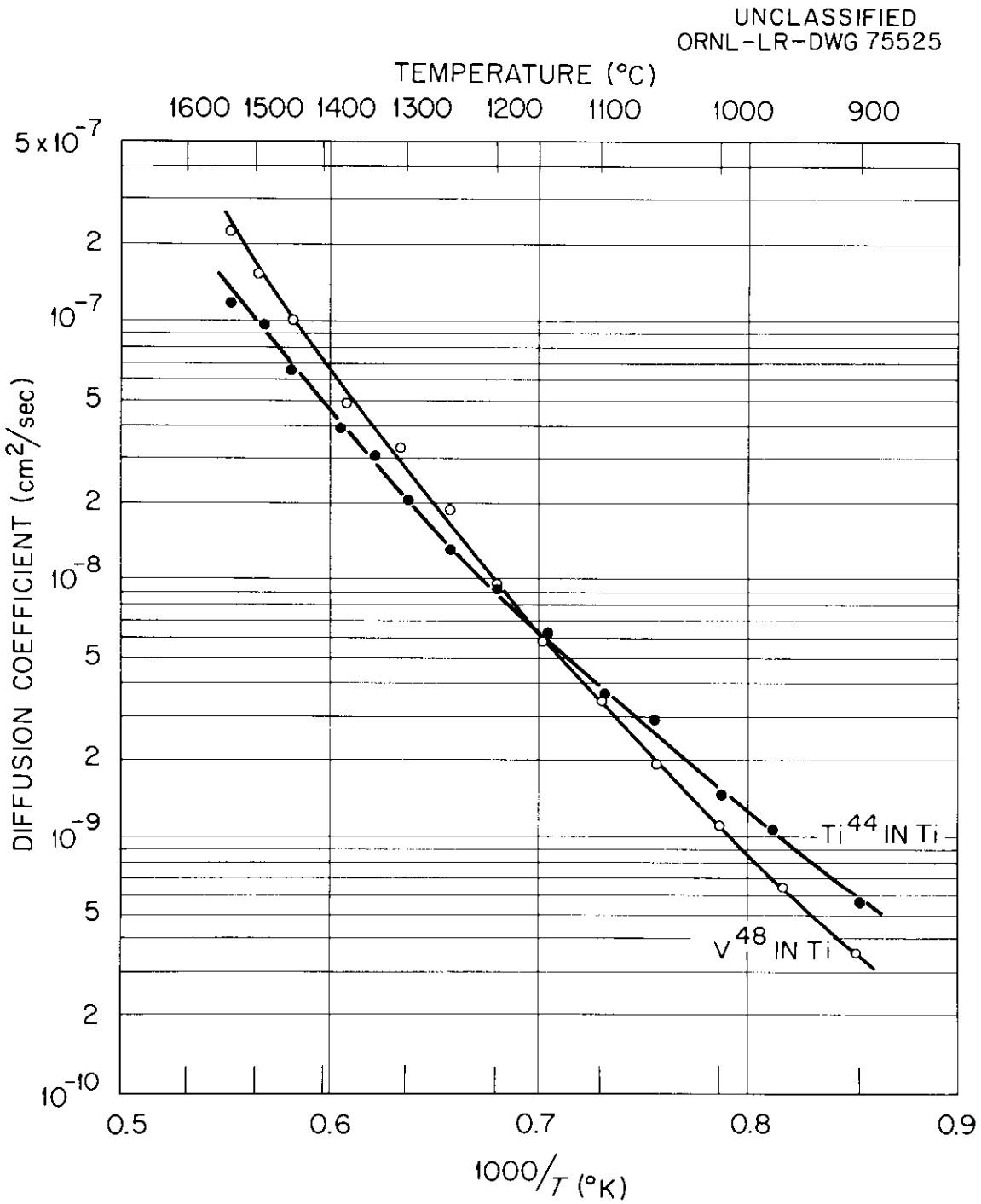

Figure 8. Temperature Dependence of the Diffusion of Titanium-44 and Vanadium-48 in Titanium.

CHAPTER V

DISCUSSION AND CONCLUSIONS

Federer and Lundy (48) and Graham (49) have discussed various methods of considering nonlinear behavior in an Arrhenius-type plot. That the plot of ln D versus 1/T results in a continuously curving line over the entire temperature range is compatible with all three of the possible explanations that have been given. These are:

1. The same diffusion mechanism may apply over the entire temperature range with the activation energy being temperature dependent. As Federer and Lundy (48) pointed out, the fact that activation energies of diffusion have previously been found constant with temperature is only an empirical fact and must be demonstrated by experiment in each instance. For diffusion in zirconium or in titanium for any sufficiently narrow temperature range, the activation energy may appear constant. Only this study and previous ones (48, 49) covering wide temperature intervals have given nonlinear ln D versus 1/T plots which suggest variations of activation energy with temperature.
2. The data at high temperatures could be considered to be that resulting from pure volume diffusion, while diffusion at low temperatures could be predominantly by short-circuit paths such as grain boundaries or dislocations. The experiments of Peart and Tomlin (46) and Graham (49) using

the autoradiographic technique tend to exclude the short-circuit mechanism as a basis for explaining the magnitude of the curvature.

3. The third idea is that the curvature may be attributed to the competition of two or more volume diffusion mechanisms. Kidson (55) has postulated that diffusion in zirconium may be divided into two regions — "extrinsic" and "intrinsic." He attributes the low-temperature "extrinsic" region to the presence of a temperature-independent concentration of vacancies due to the presence of some impurity (possibly oxygen). Further, he considers the "extrinsic" concentration of vacancies to be much greater than the concentration of thermal vacancies ("intrinsic") at low temperatures.

Kidson treated the zirconium data as the sum of two exponential terms — one representing the "extrinsic" region; the other representing the "intrinsic" region. Using this approach in the present research, the titanium-44 and vanadium-48 data were expressed as the sum of two exponential terms. A program was written for the IBM-7090 computer (see Acknowledgments, p ii) which used the method of nonlinear least squares to yield the best fit of the sum of two exponential terms to the experimental data. The computer program required an estimate of the two exponential terms as a starting point to choose the best least squares term. The estimates were obtained in the following way: The first exponential term corresponding to the "extrinsic" region was obtained by drawing a tangent to the experimental curve and calculating

the constants, Q^{ext} and D_o^{ext}. The tangent was extrapolated to the high-temperature region, and the extrapolated values of the diffusion coefficient were subtracted from the experimental data, yielding the second exponential term which represents the "intrinsic" region. The resulting computer-derived equations are:

$$D_{Ti^{44}} = 3.58 \times 10^{-4} \exp\left(-\frac{31,200}{RT}\right) + 1.09 \exp\left(-\frac{60,000}{RT}\right) \tag{5}$$

$$D_{V^{48}} = 3.10 \times 10^{-4} \exp\left(-\frac{32,200}{RT}\right) + 1.37 \exp\left(-\frac{57,200}{RT}\right) \quad . \tag{6}$$

Diffusion coefficients calculated from these equations are compared in Figures 9 and 10 with the experimental data. Each term of the sum plots linearly on a semilogarithmic scale with 1/T as the linear coordinate and the sum plots as a continuous curve.

Equations (5) and (6) are of the form

$$D = C_A \exp\left(-\frac{Q_A}{RT}\right) + C_B \exp\left(-\frac{Q_B}{RT}\right) \quad . \tag{7}$$

Differentiating the logarithm of Equation (7) with respect to 1/T yields

$$\frac{d \ln D}{d(1/T)} = \frac{-C_A \frac{Q_A}{R} \exp\left(-\frac{Q_A}{RT}\right) - C_B \frac{Q_A}{R} \exp\left(-\frac{Q_B}{RT}\right)}{C_A \exp\left(-\frac{Q_A}{RT}\right) + C_B \exp\left(-\frac{Q_B}{RT}\right)} \quad . \tag{8}$$

Multiplying Equation (8) by −R gives a parameter which was called the apparent activation energy by Federer and Lundy (48) and Kidson (55). Plots of the apparent activation energy as a function of temperature for titanium-44 and vanadium-48 diffusing in titanium are shown in

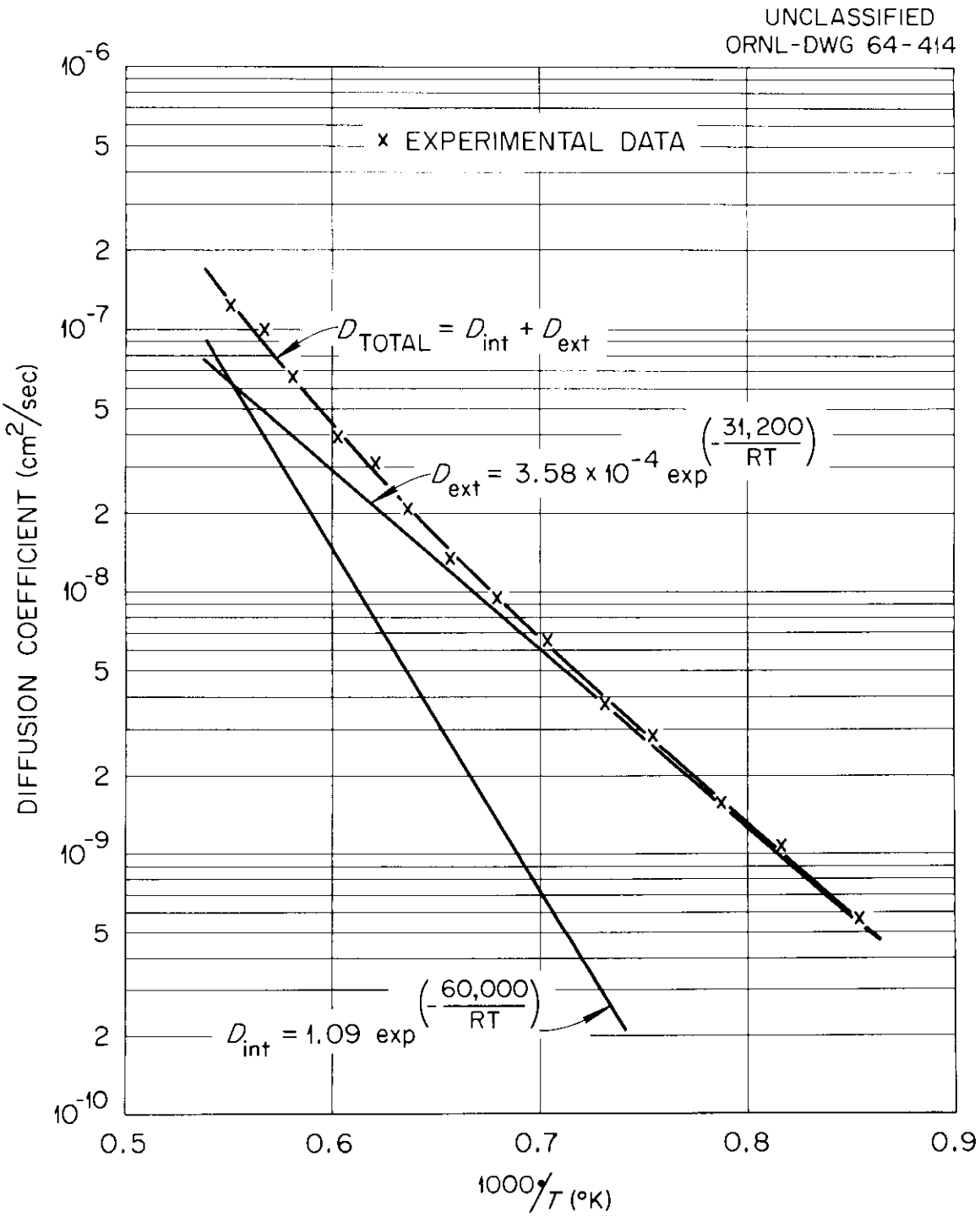

Figure 9. Computer Fit of the Experimental Data for the Diffusion of Titanium-44 in Titanium to the Model Proposed by Kidson (55).

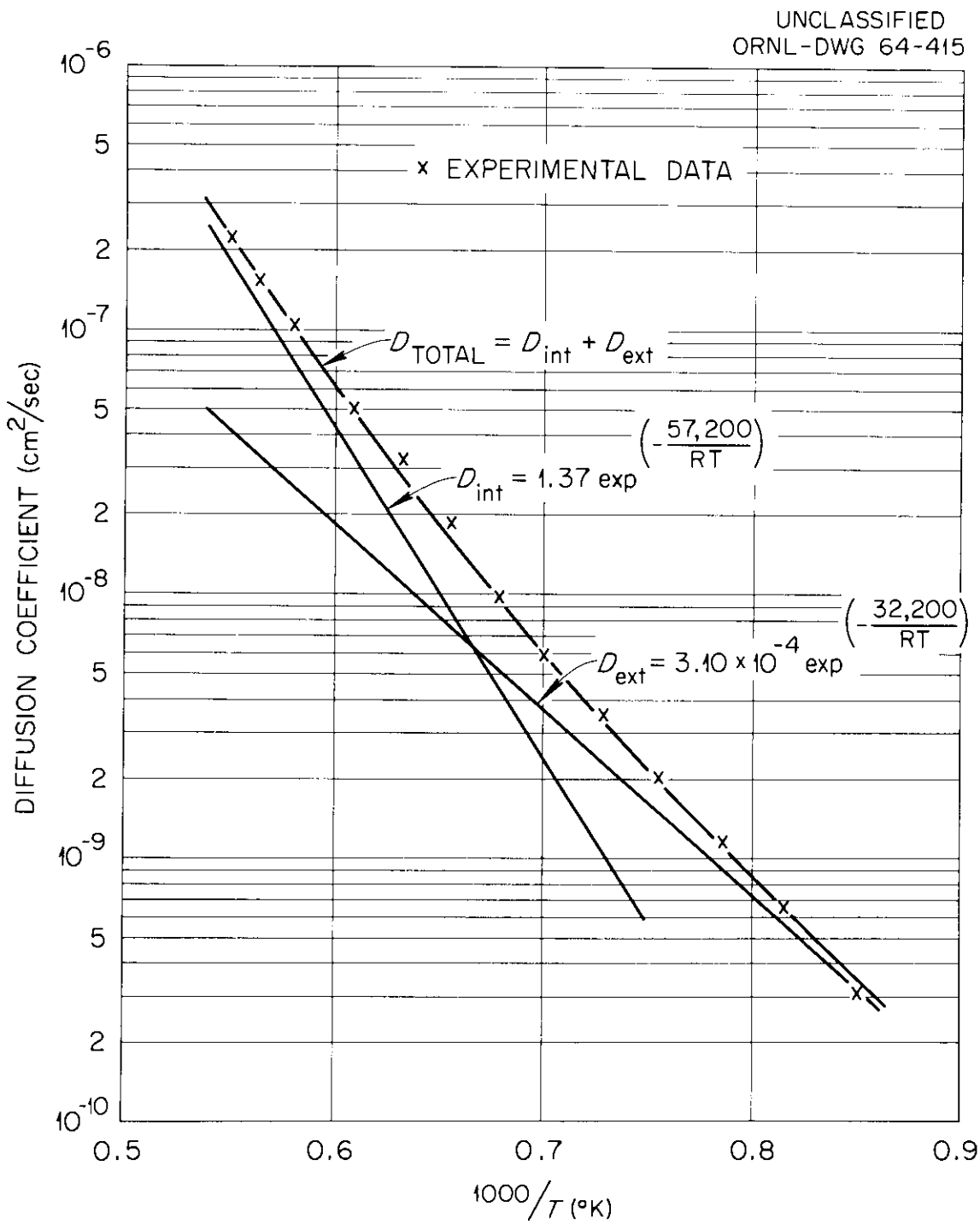

Figure 10. Computer Fit of the Experimental Data for the Diffusion of Vanadium-48 in Titanium to the Model Proposed by Kidson (55).

Figure 11. The results of Kidson's treatment of the zirconium data are shown in Figure 11, also for qualitative comparison.

In conclusion, the Arrhenius-type equation with constant D_o and Q has been shown to be inapplicable in completely describing the data for diffusion in titanium. This further substantiates the results of Federer and Lundy (48) and Graham (49).

Three possible explanations have been offered: that the activation energy is a temperature-dependent function for a single mechanism; that diffusion along short-circuit paths predominates at low temperatures; and that there may be two or more competing volume diffusion mechanisms. The proposed model of Kidson is seen to qualitatively explain the data. However, with the presently available data, no single explanation of the observed anomaly can as yet be ruled correct.

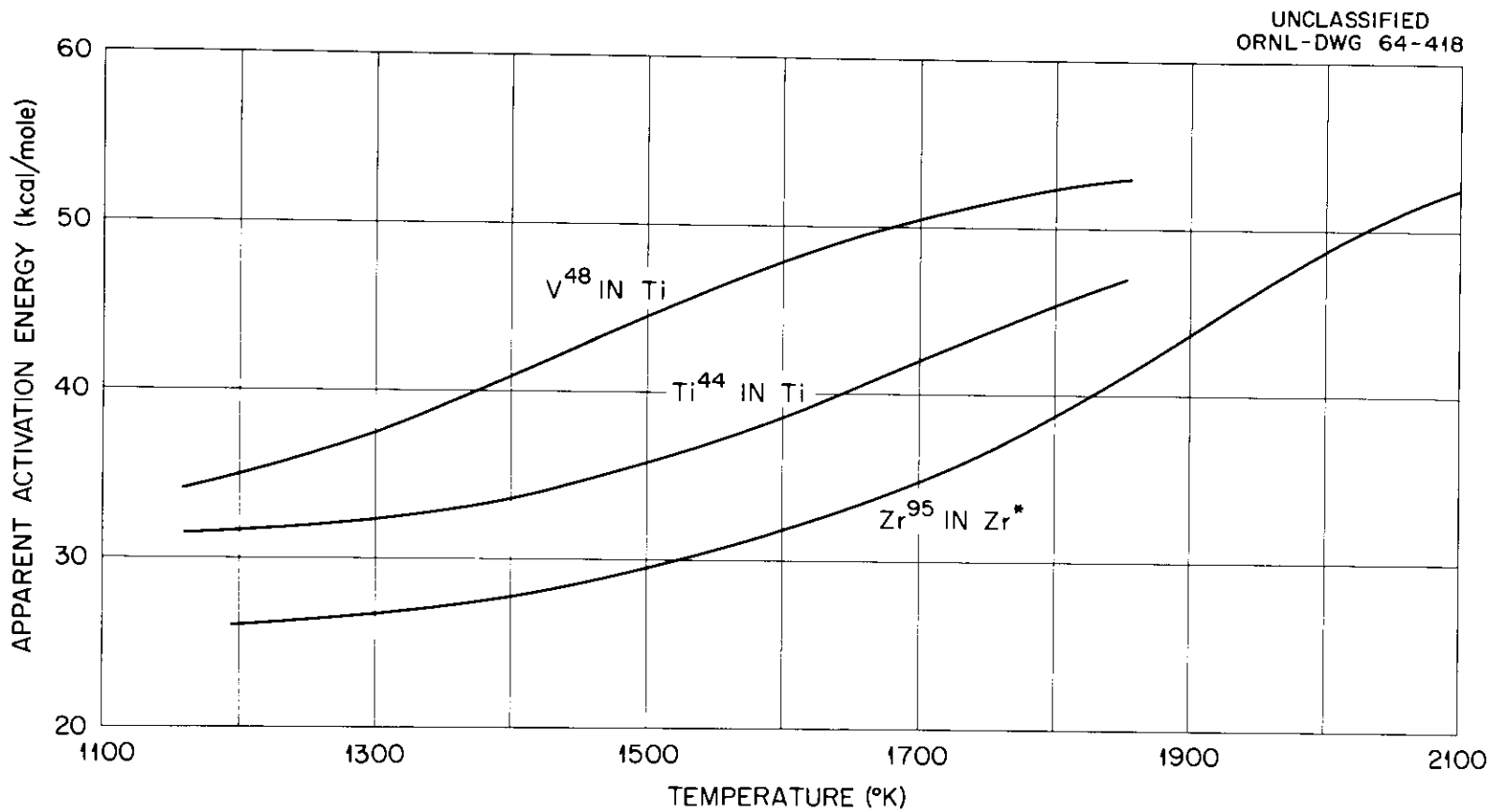

Figure 11. Temperature Dependence of the Apparent Activation Energy for the Diffusion of Titanium-44 and Vanadium-48 in Titanium and Zirconium-95 in Zirconium (55).

REFERENCES

1. Jelks Barksdale, Titanium, Its Occurrence, Chemistry, and Technology, The Ronald Press Company, New York, 1949.

2. Historical Monograph, The Ordnance Corps Titanium Program 1946-1961, February 1962.

3. Wolfgang Seith and Theodor Heumann, Diffusion of Metals: Exchange Reactions, Springer-Press, Berlin, 1955.

4. Paul G. Shewmon, Diffusion in Solids, McGraw-Hill, New York, 1963.

5. J. Crank, The Mathematics of Diffusion, Oxford University Press, London, 1957.

6. W. Jost, Diffusion in Solids, Liquids, Gases, Academic Press, New York, 1960.

7. R. E. Hoffman and D. Turnbull, "Lattice and Grain Boundary Self-Diffusion in Silver," J. Appl. Phys., 22, 634 (1951).

8. L. Slifkin, D. Lazarus, and T. Tomizuka, "Self-Diffusion in Pure Polycrystalline Silver," J. Appl. Phys., 23, 1032 (1952).

9. A. Kuper, H. Letaw, Jr., L. Slifkin, E. Sonder, and C. T. Tomizuka, "Self-Diffusion in Copper," Phys. Rev., 96, 1224 (1954).

10. E. Sonder, L. Slifkin, and C. T. Tomizuka, "Diffusion of Antimony in Silver," Phys. Rev., 93, 970 (1954).

11. C. T. Tomizuka and L. Slifkin, "Diffusion of Cadmium, Indium, and Tin in Single Crystals of Silver," Phys. Rev., 96, 610 (1954).

12. E. Sonder, "Effect of Antimony Impurity on Self-Diffusion of Silver," Phys. Rev., 100, 1662 (1955).

13. R. E. Hoffman, D. Turnbull, and E. W. Hart, "Self-Diffusion in Dilute Binary Solid Solutions," Acta Met., 3, 417 (1955).

14. A. Sawatzky and F. E. Jaumot, Jr., "Diffusion of Zinc in Single Crystals of Silver," Phys. Rev., 100, 1627 (1955).

15. W. M. Portnoy, H. Letaw, Jr., and L. Slifkin, "Self-Diffusion in Germanium," Phys. Rev., 98, 1536 (1955).

16. F. E. Jaumot, Jr., and A. Sawatzky, "Diffusion of Gold in Single Crystals of Silver," J. Appl. Phys., 27, 1186 (1956).

17. C. T. Tomizuka and E. Sonder, "Self-Diffusion in Silver," Phys. Rev., 103, 1182 (1956).

18. A. B. Kuper, D. Lazarus, J. R. Manning, and C. T. Tomizuka, "Diffusion in Ordered and Disordered Copper-Zinc," Phys. Rev., 104, 1536 (1956).

19. R. E. Hoffman, F. W. Pikus, and R. A. Ward, "Self-Diffusion in Solid Nickel," Trans. Met. Soc. AIME, 206, 483 (1956).

20. A. Sawatzky and F. E. Jaumot, Jr., "Diffusion of the Elements of the IB and IIB Subgroups in Silver," J. Metals, 9, 1207 (1957).

21. N. H. Machtrieb, J. Petit, and J. Wehrenberg, "Self-Diffusion of Silver in Silver-Palladium Alloys," J. Chem. Phys., 26, 106 (1957).

22. J. Hino, C. Tomizuka, and C. Wert, "Internal Friction and Diffusion in 31% Alpha Brass," Acta Met., 5, 41 (1957).

23. S. M. Makin, A. H. Rowe, and A. D. LeClaire, "Self-Diffusion in Gold," Proc. Phys. Soc. (London), 70, 545 (1957).

24. C. A. Mackliet, "Diffusion of Iron, Cobalt, and Nickel in Single Crystals of Pure Copper," Phys. Rev., 109, 1964 (1958).

25. R. E. Hoffman, "Diffusion in Silver Germanium and Silver Thallium Solutions," Acta Met., 6, 95 (1958).

26. C. B. Pierce and D. Lazarus, "Diffusion of Ruthenium in Single Crystals of Silver," Phys. Rev., 114, 686 (1959).

27. J. R. MacEwan, J. U. MacEwan, and L. Yaffe, "Self-Diffusion in Polycrystalline Nickel," Can. J. Chem., 37, 1623 (1959).

28. J. R. MacEwan, J. U. MacEwan, and L. Yaffe, "Diffusion of Ni^{63} in Iron, Cobalt, Nickel, and Two Iron-Nickel Alloys," Can. J. Chem., 37, 1629 (1959).

29. Herbert W. Allison and George E. Moore, "Diffusion of Tungsten in Nickel and Reaction at Interface with SrO," J. Appl. Phys., 29, 842 (1958).

30. Tokutaro Hirone and Hisao Yamamoto, "Diffusion of Cobalt into Silver," J. Phys. Soc. (Japan), 16, 455 (1961).

31. Tokutaro Hirone, Shigeto Miura, and Toshiro Suzuoka, "Diffusion of Nickel in Silver," J. Phys. Soc. (Japan), 16, 2456 (1961).

32. T. S. Lundy and J. F. Murdock, "Diffusion of Al^{26} and Mn^{54} in Aluminum," J. Appl. Phys., 33, 1671 (1962).

33. Ken-Ichi Hirano, R. P. Agarwala, B. L. Averbach, and Morris Cohen, "Diffusion in Cobalt-Nickel Alloys," J. Appl. Phys., 33, 3049 (1962).

34. Ken-Ichi Hirano, R. P. Agarwala, and Morris Cohen, "Diffusion of Iron, Nickel, and Cobalt in Aluminum," Acta Met., 10, 857 (1962).

35. David Duhl, Ken-Ichi Hirano, and Morris Cohen, "Diffusion of Iron, Cobalt and Nickel in Gold," Acta Met., 11, 1 (1963).

36. Ken-Ichi Hirano, Morris Cohen, and B. L. Averbach, "Diffusion of Iron, Cobalt, and Nickel in Silver," Acta Met., 11, 463 (1963).

37. W. C. Mallard, A. B. Gardner, Ralph F. Bass, and L. M. Slifkin, "Self-Diffusion in Silver-Gold Solid Solutions," Phys. Rev., 129, 617 (1963).

38. David Lazarus, "Diffusion in Metals," Solid State Physics, 10, 71–126, Academic Press, New York, 1960.

39. Y. Adda and A. Kirianenko, "Etude de l'Autodiffusion de l'Uranium en Phase γ," J. Nucl. Mater., 2, 120 (1959).

40. A. J. Mortlock, "Autoradiographic Investigation of the Diffusion of Chromium in Titanium," Colloque sur la Diffusion a l'Etat Solide, pp 13–16, North Holland Publishing Company, Amsterdam, 1959.

41. A. J. Mortlock and D. H. Tomlin, "The Atomic Diffusion of Chromium in the Titanium-Chromium System," Phil. Mag., 4, 628 (1959).

42. H. W. Paxton and T. Kunitake, "Diffusion in the Iron-Chromium System," Trans. Met. Soc. AIME, 218, 1003 (1960).

43. S. J. Rothman, "The Diffusion of Gold in Gamma Uranium," J. Nucl. Mater., 3, 77 (1961).

44. G. Kidson and J. McGurn, "Self-Diffusion in Body-Centered Cubic Zirconium," Can. J. Phys., 39, 1146 (1961).

45. W. C. Hagel, "Self-Diffusion in Solid Chromium," Trans. Met. Soc. AIME, 224, 430 (1962).

46. R. F. Peart and D. H. Tomlin, "Diffusion of Solute Elements in Beta-Titanium," Acta Met., 10, 123 (1962).

47. R. F. Peart, D. Graham, and D. H. Tomlin, "Tracer Diffusion in Niobium and Molybdenum," Acta Met., 10, 519 (1962).

48. J. I. Federer and T. S. Lundy, "Diffusion of Zr^{95} and Cb^{95} in Bcc Zirconium," Trans. Met. Soc. AIME, 227, 592 (1963).

49. G. B. Gibbs, D. Graham, and D. H. Tomlin, "Diffusion in Titanium and Titanium-Niobium Alloys," Phil. Mag., 8(92), 1269 (1963); D. Graham, Ph.D. Thesis, University of Reading, November 1962.

50. J. Askill and D. H. Tomlin, "Self-Diffusion in Molybdenum," Phil. Mag., 8(90), 997 (1963).

51. P. G. Shewmon and J. H. Bechtold, "Marker Movements in Titanium-Molybdenum Diffusion Couples and the Zener Theory of D_o," Acta Met., 3, 452 (1955).

52. D. Goold, "Diffusion of Aluminum, Tin, Vanadium, Molybdenum, and Manganese in Titanium," J. Inst. Metals (London), 88, 444 (1959).

53. H. W. Paxton and E. J. Pasierb, "Measurement of Kirkendall Effect in the Iron-Chromium System," Trans. Met. Soc. AIME, 218, 794 (1960).

54. R. F. Peart and D. H. Tomlin, "The Kirkendall Effect in the B.C.C. Phase of the Titanium-Chromium System," Phys. Chem. Solids, 23, 1169 (1962).

55. G. V. Kidson, "On the Anomalous Self-Diffusion in Body-Centered Cubic Zirconium," Can. J. Phys., 41, 1563 (1963).

56. William H. Sullivan, Trilinear Chart of Nuclides (2nd ed.), Oak Ridge National Laboratory, January 1957.

57. F. R. Winslow, A FORTRAN Program for Calculating Diffusion Coefficients and Plotting Penetration Curves, ORNL TM-726, Oak Ridge National Laboratory, 1963.

58. R. V. Churchill, Fourier Series and Boundary Value Problems (1st ed.), p 92, McGraw-Hill, New York, 1941.

APPENDIX A

DERIVATION OF FICK'S SECOND LAW AND SOLUTION FOR PLANE SOURCE SEMI-INFINITE GEOMETRY

From the first equation of Fick,

$$F_x = -D\ \partial c/\partial x \quad , \tag{9}$$

the second equation,

$$\frac{\partial c}{\partial t} = D\ \frac{\partial^2 c}{\partial x^2} \quad , \tag{10}$$

is developed by considering an elemental volume (Figure 12) with sides 2 dx, 2 dy, and 2 dz (5). The concentration, c, of the diffusing species applies at the center P (x,y,z) of this element of volume. If ABCD and A′B′C′D′ are the plane faces of the volume normal to the x axis, then the flow through the face ABCD is

$$N_x = 4\ dydz \left(F_x - \frac{\partial F_x}{\partial x}\ dx\right) \ , \tag{11}$$

where F_x is the flux through the plane which is normal to the x axis containing P(x,y,z). The flow through the plane A′B′C′D′ is

$$N_x' = 4\ dydz \left(F_x + \frac{\partial F_x}{\partial x}\ dx\right) \ . \tag{12}$$

The rate of accumulation of the diffusing species in the elemental volume due to the net flow across these two faces is the difference of Equation (11) and Equation (12) or

UNCLASSIFIED
ORNL-DWG 64-1510

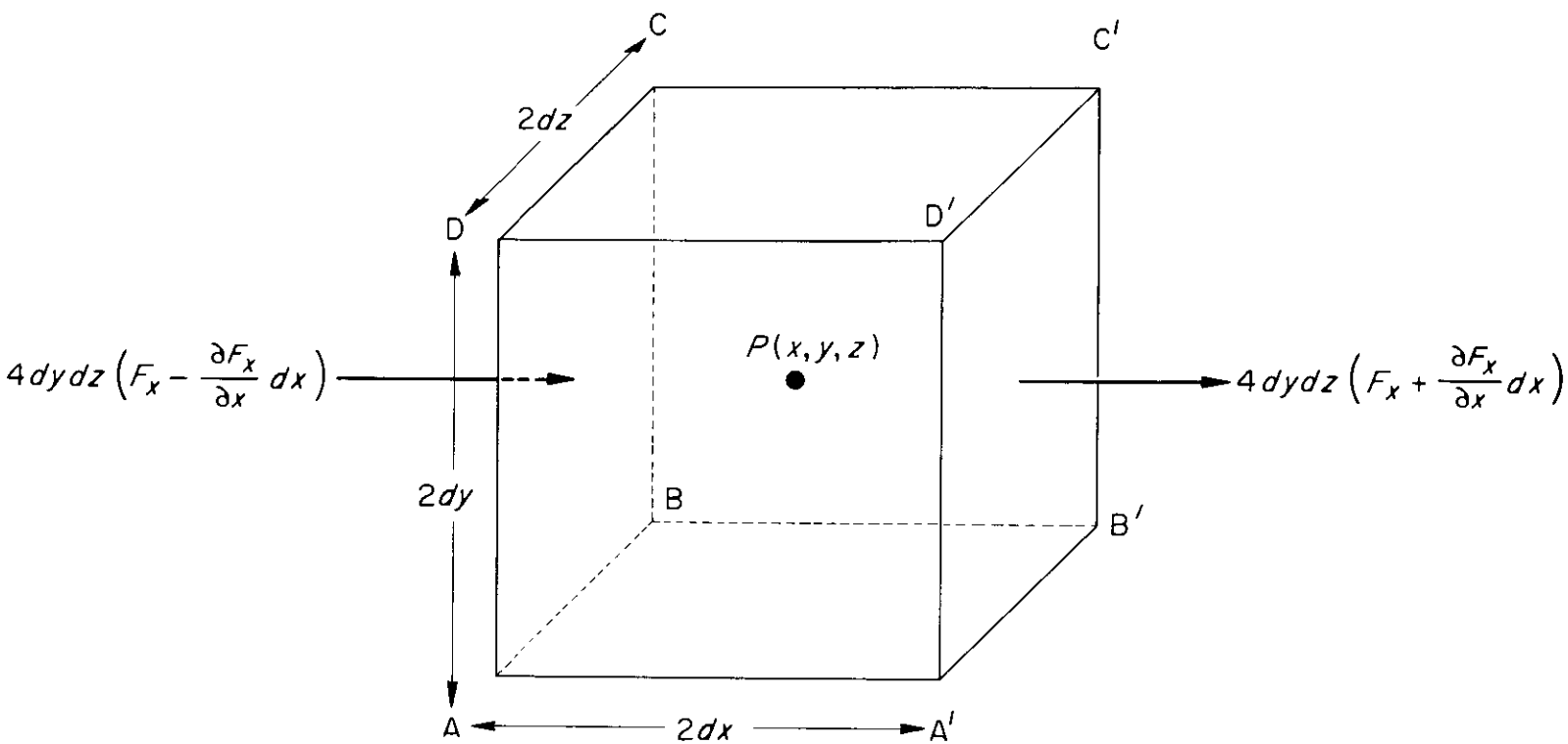

Figure 12. Differential Element of Volume.

$$N_x - N_x' = -8\ dxdydz\ \frac{\partial F_x}{\partial x} \quad . \tag{13}$$

In a like manner, the accumulations due to the net flow across the other faces are

$$N_y - N_y' = -8\ dxdydz\ \frac{\partial F_y}{\partial y} \quad \text{and} \quad N_z - N_z' = -8\ dxdydz\ \frac{\partial F_z}{\partial z} \quad . \tag{14}$$

But the accumulation in the volume is also

$$N = 8\ dxdydz\ \frac{\partial c}{\partial t} \quad ; \tag{15}$$

and, upon equating the sum of Equations (13) and (14) to Equation (15), the relationship between concentration and the flux at the faces becomes

$$\frac{\partial c}{\partial t} + \frac{\partial F_x}{\partial x} + \frac{\partial F_y}{\partial y} + \frac{\partial F_z}{\partial z} = 0 \tag{16}$$

which, upon substitution of Equation (9), yields

$$\frac{\partial c}{\partial t} - \frac{\partial\left(D\ \frac{\partial c}{\partial x}\right)}{\partial x} - \frac{\partial\left(D\ \frac{\partial c}{\partial y}\right)}{\partial y} - \frac{\partial\left(D\ \frac{\partial c}{\partial z}\right)}{\partial z} = 0 \quad . \tag{17}$$

If the diffusion coefficient is constant, Equation (17) simplifies to

$$\frac{\partial c}{\partial t} = D\left(\frac{\partial^2 c}{\partial x^2} + \frac{\partial^2 c}{\partial y^2} + \frac{\partial^2 c}{\partial z^2}\right) \tag{18}$$

reducing to

$$\frac{\partial c}{\partial t} = D\ \frac{\partial^2 c}{\partial x^2} \tag{19}$$

if there is a concentration gradient along the x axis only.

Equation (19) must be solved for $c = f(x,t)$ for $0 < x < \infty$ and all t subject to boundary conditions:

$$\frac{\partial c(0,t)}{\partial x} = 0 \tag{20}$$

for $t > 0$, or there is no diffusion across the open face, and $c(x,\infty)$ remains finite as $t \to \infty$ and subject to the initial condition:

$$c(x,0) = f(x) \quad . \tag{21}$$

Assume the solution $c(x,t)$ to be a product of a function of distance, $X(x)$, and a function of time, $T(t)$,

$$c(x,t) = X(x) \cdot T(t) \quad . \tag{22}$$

Substituting Equation (22) in Equation (18) gives

$$XT' = DTX'' \tag{23}$$

if D is constant. The primes denote differentiation with respect to the appropriate variables.

Separating variables yields

$$\frac{T'}{T} = D\,\frac{X''}{X} \quad . \tag{24}$$

Since the variables are separable such that the left side of Equation (24) is a function of t only and the right side is a function of x only, it follows that each side is constant, independent of both x and t. Arbitrarily choosing the constant to be $-p^2D$ yields solutions to the two ordinary differential equations resulting from Equation (24),

$$T \cong \exp\,(-p^2Dt) \text{ and } X = a\cos px + b\sin px \quad . \tag{25}$$

If the solution is to remain finite, a restriction $p^2 > 0$ must be made.

Then

$$c(x,t) = [a\cos px + b\sin px]\,\exp\,(-p^2Dt) \quad . \tag{26}$$

Differentiating with respect to x

$$\frac{\partial c(x,t)}{\partial x} = [-ap\sin px + bp\cos px]\,\exp\,(-p^2Dt) \tag{27}$$

and applying boundary condition, Equation (19) yields

$$\frac{\partial c(0,t)}{\partial x} = [-0 + bp]\,\exp\,(-p^2Dt) = 0 \tag{28}$$

or $b = 0$. Therefore

$$c(x,t) = a\cos px\,\exp\,(-p^2Dt) \quad . \tag{29}$$

A single term of this form could not, in general, fit Condition (21). However, over the interval from $0 < x < \infty$ a function, $f(x)$, can be represented by the Fourier cosine integral (58)

$$f(x) = \frac{2}{\pi}\int_0^\infty \cos\alpha x d\alpha \int_0^\infty f(x')\,\cos\alpha x'\,dx' \tag{30}$$

which places the solution in Fourier integral form by taking

$$a = f(x')\,\cos px'\,dp dx' \tag{31}$$

and integrating over $0 < p < \infty$, $0 < x' < \infty$. Note that the right-hand side of Equation (31) is not a function of x or t. Thus

$$c(x,t) = \frac{2}{\pi} \int_0^\infty \cos px \exp(-p^2Dt)\, dp \int_0^\infty f(x')\cos px'\, dx' \tag{32}$$

and, in particular,

$$c(x,0) = f(x) = \frac{2}{\pi} \int_0^\infty \cos px\, dp \int_0^\infty f(x')\cos px'\, dx' \quad . \tag{33}$$

Now

$$\cos\alpha \cos\beta = \frac{1}{2}[\cos(\alpha+\beta) + \cos(\alpha-\beta)] \quad , \tag{34}$$

so the solution can be written

$$c(x,t) = \frac{1}{\pi} \int_0^\infty \int_0^\infty f(x')\,[\cos p(x'+x) + \cos p(x'-x)] \exp(-p^2Dt)\, dp\, dx' \quad . \tag{35}$$

Integrate first with respect to p as follows. Let

$$p^2Dt = \eta^2 \ , \ \frac{x'+x}{\sqrt{Dt}} = \xi \ , \text{ and } \frac{x'-x}{\sqrt{Dt}} = \xi'$$

then

$$p = \frac{\eta}{\sqrt{Dt}} \ , \ dp = \frac{d\eta}{\sqrt{Dt}} \ , \text{ and } p(x'+x) = \xi\eta$$

and

$$\int_0^\infty \cos p(x'+x) \exp(-p^2Dt)\, dp = \frac{1}{\sqrt{Dt}} \int_0^\infty \cos\xi\eta \exp(-\eta^2)\, d\eta = g(\xi) \quad . \tag{36}$$

Differentiating Equation (36) with respect to ξ yields

$$\frac{dg(\xi)}{d\xi} = \frac{1}{\sqrt{Dt}} \int_0^\infty (-\eta \sin\xi\eta) \exp(-\eta^2)\, d\eta \quad . \tag{37}$$

Integrate Equation (37) by parts with $u = \sin\xi\eta$, $du = \xi \cos\xi\eta d\eta$,

$dv = -\eta \exp(-\eta^2)d\eta$, and $v = \dfrac{\exp(-\eta^2)}{2}$; then

$$\frac{dg(\xi)}{d\xi} = \frac{1}{\sqrt{Dt}} \left\{ \left[\frac{\exp(-\eta^2) \sin\xi\eta}{2} \right]_0^\infty - \frac{\xi}{2} \int_0^\infty \cos\xi\eta \exp(-\eta^2)\, d\eta \right\} \quad . \tag{38}$$

Recalling Equation (36) gives

$$\frac{dg(\xi)}{d\xi} = -\frac{\xi}{2}\, g(\xi) \quad . \tag{39}$$

Integrating Equation (39)

$$\int_{g_o}^{g(\xi)} \frac{dg(\xi)}{g(\xi)} = -\int_0^{\xi} \frac{\xi}{2}\, d\xi$$

where $g_o = g(o)$, and

$$\ln \frac{g(\xi)}{g_o} = -\frac{\xi^2}{4} \quad \text{or} \quad g(\xi) = g_o \exp\,(-\xi^2/4) \quad . \tag{40}$$

From its definition

$$g_o = \frac{1}{\sqrt{Dt}} \int_0^{\infty} \exp\,(-\eta^2)\, d\eta = \frac{1}{2}\sqrt{\pi/Dt}$$

so

$$g(\xi) = \frac{1}{2}\sqrt{\pi/Dt}\, \exp\,(-\xi^2/4) \quad . \tag{41}$$

Similarly

$$g(\xi') = \frac{1}{2}\sqrt{\pi/Dt}\, \exp\,(-\xi'^2/4) \tag{42}$$

so that

$$c(x,t) = \frac{1}{2\sqrt{\pi Dt}} \int_0^{\infty} f(x')\, \left\{ \exp\left[-\frac{(x'+x)^2}{4Dt}\right] + \exp\left[-\frac{(x'-x)^2}{4Dt}\right] \right\} dx' \tag{43}$$

which holds for any initial distribution in semi-infinite geometry.

For a "plane source" initial condition, $f(x) = 0$ for $x > 0$ and $\int_0^{\infty} f(x)\, dx = M$, the amount of diffusing species per unit surface area.

This is equivalent to stating that $f(x)$ is given by the limit as $\epsilon \to 0$ of the function $h(x)$ defined by

$$\left.\begin{aligned} h(x) &= \frac{M}{\epsilon}, \ x < \epsilon \\ h(x) &= 0, \ x > \epsilon \end{aligned}\right\} \quad . \tag{44}$$

Note that

$$\int_0^\infty h(x)dx = \int_0^\epsilon \frac{M}{\epsilon}\, dx + \int_\epsilon^\infty 0 \cdot dx = \frac{M}{\epsilon} \cdot \epsilon = M \quad .$$

Then

$$c(x,t) = \lim_{\epsilon \to 0} \left\{ \frac{1}{2\sqrt{\pi Dt}} \int_0^\infty h(x') \left(\exp\left[\frac{-(x'-x)^2}{4Dt}\right] + \exp\left[\frac{-(x'+x)^2}{4Dt}\right] \right) dx' \right\}$$

$$= \lim_{\epsilon \to 0} \left\{ \frac{1}{2\sqrt{\pi Dt}} \int_0^\epsilon \frac{M}{\epsilon} \left(\exp\left[\frac{-(x'-x)^2}{4Dt}\right] + \exp\left[\frac{-(x'+x)^2}{4Dt}\right] \right) dx' \right.$$

$$\left. + \frac{1}{2\sqrt{\pi Dt}} \int_\epsilon^\infty 0 \cdot dx' \right\} \quad . \tag{45}$$

Since $x' > \epsilon$ in the first integral, $x' - x \approx x' + x \approx x$, then

$$c(x,t) = \lim_{\epsilon \to 0} \left\{ \frac{1}{2\sqrt{\pi Dt}} \int_0^\infty \frac{M}{\epsilon} \cdot 2 \exp\left(\frac{-x^2}{4Dt}\right) dx' \right\} = \frac{\exp(-x^2/4Dt)}{\sqrt{\pi Dt}} \lim_{\epsilon \to 0} \int_0^\epsilon \frac{M}{\epsilon}\, dx'$$

yielding finally

$$c(x,t) = \frac{M}{\sqrt{\pi Dt}} \exp\left(\frac{-x^2}{4Dt}\right) \quad , \tag{46}$$

which is the solution needed for the conditions of this experiment.

APPENDIX B

SECULAR EQUILIBRIUM

Consider an isotope decay chain of a radioactive parent decaying to a radioactive daughter. Two competing processes control the amount of the daughter species: the rate of decay of the parent which is the source on one side and the rate of decay of the daughter which is the sink on the other side. The purpose of this Appendix is to treat mathematically the consequences of these competing processes.

Defining:

N_1 = amount of parent present at any time, t

N_2 = amount of daughter present at any time, t

T_1 and T_2 = half-life of parent and daughter, respectively

λ_1 and $\lambda_2 = \frac{\ln 2}{T_1}$ and $\frac{\ln 2}{T_2}$ = respective decay constants of parent and daughter.

In general for a large number of radioactive atoms of any one species, the rate of decay of the species is proportional to the number of atoms present.

$$\frac{dN}{dt} = -\lambda N \quad . \tag{47}$$

The negative sign arises because the rate decreases with time.

Integration of Equation (47) gives

$$N = N^o \, e^{-\lambda t} \tag{48}$$

where N^o is the number of atoms at time, t = 0. Then the rate of accumulation of the daughter species is

$$\frac{dN_2}{dt} = -\frac{dN_1}{dt} - \lambda_2 N_2 \quad . \tag{49}$$

Substituting Equation (47) in Equation (49) gives

$$\frac{dN_2}{dt} = \lambda_1 N_1 - \lambda_2 N_2 \tag{50}$$

but

$$N_1 = N_1^o \, e^{-\lambda_1 t} \quad , \tag{51}$$

so

$$\frac{dN_2}{dt} = \lambda_1 N_1^o \, e^{-\lambda_1 t} - \lambda_2 N_2 \quad . \tag{52}$$

Equation (52) is of the form

$$y' + ay = c \, e^{bx} \tag{53}$$

which has solutions

$$y = \frac{c}{a+b} \, e^{bx} + K \, e^{-ax} \tag{54}$$

for $a + b \neq 0$, and

$$y = cx \, e^{bx} + K \, e^{-ax} \tag{55}$$

for $a + b = 0$.

Let $N_2 = y$, $t = x$, $a = \lambda_2$, $b = -\lambda_1$, and $c = \lambda_1 N_1^o$. Then

$$N_2 = \frac{\lambda_1 N_1^o}{\lambda_2 - \lambda_1} \, e^{-\lambda_1 t} + K \, e^{-\lambda_2 t} \tag{56}$$

for $\lambda_2 \neq \lambda_1$, and

$$N_2 = \lambda_1 N_1^o \, t \, e^{-\lambda_1 t} + K \, e^{-\lambda_2 t} \tag{57}$$

for $\lambda_2 = \lambda_1$. If $N_2 = 0$ at $t = 0$, Equation (56) becomes

$$N_2 = \frac{\lambda_1 N_1^o \, e^{-\lambda_1 t}}{\lambda_2 - \lambda_1} - \frac{\lambda_1 N_1^o \, e^{-\lambda_2 t}}{\lambda_2 - \lambda_1} \tag{58}$$

and Equation (57) becomes

$$N_2 = \lambda_1 N_1^o \, t \, e^{-\lambda_1 t} = \lambda_1 N_1^o \, t \, e^{-\lambda_2 t} \tag{59}$$

or upon recalling Equation (51)

$$N_2 = \lambda_1 N_1 t \quad . \tag{60}$$

Consider now Equation (58) when $T_1 >> T_2$ then N_1 can be considered constant and $\lambda_2 >> \lambda_1$ so that

$$N_2 = \frac{\lambda_1 N_2}{\lambda_2} - \frac{\lambda_1 N_1}{\lambda_2} \, e^{-\lambda_2 t} \tag{61}$$

or

$$\frac{N_2}{N_1} = \frac{\lambda_1}{\lambda_2}\left(1 - e^{-\lambda_2 t}\right) \quad . \tag{62}$$

For a sufficiently large time, Equation (62) becomes

$$\frac{N_2}{N_1} = \frac{\lambda_1}{\lambda_2} = \text{constant.} \tag{63}$$

Equation (63) describes the state of secular equilibrium where the ratio of the amount of the daughter species to the parent species is constant.

Since $\frac{N_2}{N_1} = f\left(\frac{1}{e^t}\right)$, the condition where $\frac{N_2}{N_1} = c$ is never reached so that the fraction $\left(1 - e^{-\lambda_2 t}\right)$ must be examined to determine the departure from secular equilibrium. For titanium-44, T = 1000 years and for scandium-44, T = 3.96 hours or $\lambda_{Ti} = 2.197 \times 10^{-11}$ sec^{-1} and $\lambda_{Sc} = 4.863 \times 10^{-5}$ sec^{-1}. After four days, $e^{-\lambda_{Sc} t} = 5.06 \times 10^{-8}$ or the per cent departure from secular equilibrium is 5.06×10^{-6} .

APPENDIX C

TABLE IV. EXPERIMENTAL DATA AND SAMPLE CALCULATION

Annealing temperature (°C)	Section number[a]	Gross weight (g)	Tare weight (g)	Activity (counts)	Counting time (sec)	Annealing time (sec)	Thermal expansion $\Delta L/L$	Specimen diameter (inch)
						$\times 10^4$		
1053	T5-1	11.92107	11.90134	4032	1200	7.02	0.00874	0.5496
	-2	12.55107	12.51811	4112	770			
	-3	12.57348	12.53900	10,353	1850			
	-4	12.61443	12.58122	4468	850			
	-5	12.65065	12.61676	4092	900			
	-6	12.66202	12.62991	4051	1200.3			
	-7	12.76436	12.72625	4046	1360			
	-8	12.82225	12.78948	4707	2520			
	-9	12.84597	12.80725	4023	2570			
Background				2053	3600			
1093.5	T6-1	13.01346	12.98121	6703	1600	6.66	0.00914	0.5496
	-2	13.20583	13.16677	4256	870.2			
	-3	13.29315	13.25495	4063	900			
	-4	13.35106	13.32086	4017	1170			
	-5	13.58966	13.55584	4718	1520			
	-6	13.27355	13.23935	4423	1590			
	-7	13.28759	13.25333	4026	1930			
	-8	13.37088	13.33276	4545	2640			
	-9	13.41333	13.38224	2198	1860.1			
	-10	13.44253	13.40745	1609	1640			
Background				2846	5220			

TABLE IV (continued)

Annealing temperature (°C)	Section number[a]	Gross weight (g)	Tare weight (g)	Activity (counts)	Counting time (sec)	Annealing time (sec)	Thermal expansion $\Delta L/L$	Specimen diameter (inch)
						$\times 10^4$		
996.9	T7-1	12.47699	12.44840	7542	1210	8.64	0.00816	0.5496
	-2	12.50717	12.46951	4077	520			
	-3	12.69146	12.65940	5117	850			
	-4	12.73002	12.69307	4595	880			
	-5	12.79707	12.76631	4640	1440			
	-6	12.88220	12.84305	4955	1840.1			
	-7	12.89566	12.86054	3028	1850			
	-8	13.07393	13.06190	1584	1540			
Background				3258	5820			
898.9	T8-1	11.94950	11.90132	9061	970	16.92	0.00744	0.5496
	-2	12.55139	12.51810	4101	740.2			
	-3	12.57488	12.53899	5649	1270			
	-4	12.61505	12.58113	4096	1390			
	-5	12.65653	12.61673	4018	1910			
	-6	12.66338	12.62989	1852	1600			
Background				3258	5820			
960	T9-1	12.46030	12.44839	2842	1200	17.19	0.00780	0.5496
	-2	12.50260	12.46949	3667	650			
	-3	12.69685	12.65939	5729	950			
	-4	12.72815	12.69309	12,318	2560			
	-5	12.80000	12.76630	4925	1310			
	-6	12.87797	12.84305	3966	1300.1			
	-7	12.89677	12.86055	4868	2140			
	-8	13.08330	13.04558	3191	1930			
	-9	13.09097	13.05781	2471	2200			

TABLE IV (continued)

Annealing temperature (°C)	Section number[a]	Gross weight (g)	Tare weight (g)	Activity (counts)	Counting time (sec)	Annealing time (sec)	Thermal expansion $\Delta L/L$	Specimen diameter (inch)
						$\times 10^4$		
960	T9-10	13.10017	13.06183	1379	1580		0.00780	0.5496
Background				1087	2160			
1148	T10-1	13.25402	13.23934	4348	2150	5.760	0.00972	0.5492
	-2	13.28912	13.25329	3961	1000			
	-3	13.36645	13.33277	5791	1510			
	-4	13.41685	13.38223	6492	1710			
	-5	13.44598	13.40742	4159	1140			
	-6	11.93360	11.90133	4034	1400			
	-7	12.55385	12.51812	6891	2520			
	-8	12.57390	12.53902	5739	2560			
	-9	12.61639	12.58122	4321	2400			
	-10	12.65252	12.61681	3513	2430			
	-11	12.66656	12.62992	2897	2450			
Background				1901	3850			
1540	T19-1	11.92080	11.90134	3861	1430	0.360	0.01368	0.5498
	-2	12.55477	12.51810	3831	900			
	-3	12.57164	12.53900	3609	1000			
	-4	12.61300	12.58120	3944	1170			
	-5	12.65576	12.61678	3778	1000			
	-6	12.65295	12.62989	4028	1850			
	-7	12.75888	12.72624	4234	1620.1			
	-8	12.83491	12.78947	3928	1350			
	-9	12.83851	12.80723	3518	2000			
	-10	12.86549	12.83792	2263	1600			
	-11	13.27464	13.23934	2328	1630			
Background				1326	2700			

TABLE IV (continued)

Annealing temperature (°C)	Section number[a]	Gross weight (g)	Tare weight (g)	Activity (counts)	Counting time (sec)	Annealing time (sec)	Thermal expansion $\Delta L/L$	Specimen diameter (inch)
						$\times 10^4$		
1249	T15-1	12.47044	12.44838	3976	670	1.620	0.01072	0.5490
	-2	12.50921	12.46948	3889	400			
	-3	12.68705	12.65940	4375	690.1			
	-4	12.72685	12.69306	3967	580			
	-5	12.80178	12.76629	3934	660			
	-6	12.87902	12.84300	4460	970			
	-7	12.89020	12.86048	3771	1220			
	-8	13.09287	13.04563	3817	1200			
	-9	13.08164	13.05785	2468	1820			
	-10	13.09688	13.06190	1289	1030			
Background				1538	3000			
1450	T16-1	12.47701	12.44841	5338	760	0.480	0.01278	0.5497
	-2	12.50594	12.46949	5371	620.1			
	-3	12.69463	12.65943	6596	840			
	-4	12.73198	12.69309	4966	660			
	-5	12.79764	12.76632	5320	1000			
	-6	12.87642	12.84305	4840	1000			
	-7	12.90151	12.86054	4073	900			
	-8	13.07680	13.04566	5164	1820			
	-9	13.09545	13.05788	3423	1350			
	-10	13.10533	13.06197	3667	1860			
	-11	13.09684	13.06875	2796	2460			
	-12	13.12930	13.09181	2089	2030			
Background				1461	3000			

TABLE IV (continued)

Annealing temperature (°C)	Section number[a]	Gross weight (g)	Tare weight (g)	Activity (counts)	Counting time (sec)	Annealing time (sec)	Thermal expansion $\Delta L/L$	Specimen diameter (inch)
						$\times 10^4$		
1300	T14-1	11.93559	11.90130	6064	909.9	0.984	0.01124	0.5497
	-2	12.55616	12.51808	4257	600			
	-3	12.57034	12.53894	4025	780			
	-4	12.61679	12.58118	3811	780			
	-5	12.65192	12.61673	7767	2040			
	-6	12.66604	12.62989	3995	1339.9			
	-7	12.75469	12.72622	3466	1920			
	-8	12.83469	12.78945	2767	1500			
	-9	12.84120	12.80723	56,734	54,080			
Background				1006	2080			
1385	T13-1	12.46853	12.44835	4295	1720	0.522	0.01210	0.5486
	-2	12.50402	12.46947	4113	1150			
	-3	12.69004	12.65939	7995	2670			
	-4	12.73246	12.69305	3963	1220			
	-5	12.80473	12.76627	4286	1610			
	-6	12.87686	12.84302	3767	2019.8			
	-7	12.89498	12.86050	9616	6260			
	-8	13.08391	13.04563	3443	2800			
	-9	13.09254	13.05783	2451	2700			
Background				1023	2000			
1337	T17-1	12.47436	12.44837	4007	792	0.720	0.01160	0.5496
	-2	12.50287	12.46948	14,797	2261			
	-3	12.69283	12.65941	4006	654			
	-4	12.72399	12.69304	4036	822			
	-5	12.80132	12.76629	4004	846			
	-6	12.87874	12.84302	4003	1074			

TABLE IV (continued)

Annealing temperature (°C)	Section number[a]	Gross weight (g)	Tare weight (g)	Activity (counts)	Counting time (sec)	Annealing time (sec)	Thermal expansion $\Delta L/L$	Specimen diameter (inch)
						$\times 10^4$		
1337	T17-7	12.89459	12.86051	4089	1521		0.01160	0.5496
	-8	13.07768	13.04561	4694	2432			
	-9	13.09455	13.05785	3324	2050			
	-10	13.09569	13.06189	3329	3010			
Background				2514	5077			
1489	T18-1	11.91439	11.90130	3539	1607.4	0.378	0.01316	0.5042
	-2	12.54390	12.51807	4016	1114.6			
	-3	12.57366	12.53897	4979	1024.5			
	-4	12.60398	12.58117	4831	1581.8			
	-5	12.64686	12.61672	4107	1195.8			
	-6	12.65780	12.62989	4025	1345			
	-7	12.75373	12.72623	6923	2750.7			
	-8	12.81885	12.78945	4343	1972.5			
	-9	12.83493	12.80721	4387	2400			
	-10	12.86595	12.83790	4326	2897.3			
	-11	13.27099	13.23923	3557	2683.5			
	-12	13.28032	13.25322	1193	1200			
Background				1225	2472			
1200	T20-1	12.48400	12.44835	4421	509	2.358	0.01023	0.5495
	-2	12.49897	12.46945	4030	568.9			
	-3	12.69513	12.65940	4029	525			
	-4	12.72733	12.69304	4020	632			
	-5	12.80298	12.76627	4014	730.8			
	-6	12.87874	12.84302	4006	944			
	-7	12.89370	12.86049	4017	1414.4			
	-8	13.07846	13.04563	4014	1949.6			

TABLE IV (continued)

Annealing temperature (°C)	Section number[a]	Gross weight (g)	Tare weight (g)	Activity (counts)	Counting time (sec)	Annealing time (sec)	Thermal expansion $\Delta L/L$	Specimen diameter (inch)
						$\times 10^4$		
1200	T20-9	13.09027	13.05783	3078	1950		0.01023	0.5495
	-10	13.09709	13.06190	4005	3358.6			
Background				1204	2460			
901.5	T 24-1	11.92338	11.90133	4635	300	34.57	0.00744	0.5500
	-2	12.55710	12.51809	4198	200			
	-3	12.57449	12.53901	4116	260			
	-4	12.61572	12.58120	4105	360			
	-5	12.65436	12.61673	4119	480			
	-6	12.67036	12.62991	4036	750			
	-7	12.75452	12.72626	4020	1820			
	-8	12.82593	12.78948	6672	3900			
	-9	12.84672	12.80724	2538	2500			
	-10	12.87078	12.83790	3636	5710			
	-11	13.27592	13.23925	1613	2950			
Background				922	2000			
952	T25-1	13.10834	13.06860	5051	310	17.35	0.00770	0.5495
	-2	13.12527	13.09174	4096	340			
	-3	13.13258	13.10279	4358	500			
	-4	13.15323	13.11960	4070	550			
	-5	13.24250	13.20847	4521	900			
	-6	13.27406	13.23921	4117	1300			
	-7	13.29158	13.25318	2702	1400.1			
	-8	13.36427	13.33268	1709	1620			
Background				1138	2340			

TABLE IV (continued)

Annealing temperature (°C)	Section number[a]	Gross weight (g)	Tare weight (g)	Activity (counts)	Counting time (sec)	Annealing time (sec)	Thermal expansion $\Delta L/L$	Specimen diameter (inch)
						$\times 10^4$		
999.5	T26-1	11.93872	11.90128	4715	260	12.61	0.00820	0.5499
	-2	12.55274	12.51802	4411	300			
	-3	12.57326	12.53896	4238	360			
	-4	12.61620	12.58113	7735	810			
	-5	12.65155	12.61667	6643	1030			
	-6	12.66453	12.62983	4054	900			
	-7	12.76107	12.72620	4409	1560			
	-8	12.83042	12.78942	6163	3240			
Background				1719	3600			
1050	T27-1	12.47578	12.44835	4164	200	7.206	0.00874	0.5500
	-2	12.50490	12.46941	4097	220			
	-3	12.69458	12.65940	4082	260			
	-4	12.72671	12.69300	4038	360			
	-5	12.80154	12.76625	4097	460			
	-6	12.87946	12.84297	5862	990			
	-7	12.89648	12.86046	12,603	3360			
	-8	13.08373	13.04552	2744	1200			
	-9	13.09282	13.05775	1270	1000			
	-10	13.09101	13.06183	833	1000			
Background				623	1300			
1099	T28-1	11.93818	11.90129	4034	250	6.480	0.00920	0.5501
	-2	12.55427	12.51807	4135	310			
	-3	12.57443	12.53899	4040	350			
	-4	12.61412	12.58114	4064	450			
	-5	12.65814	12.61671	4058	450			

TABLE IV (continued)

Annealing temperature (°C)	Section number[a]	Gross weight (g)	Tare weight (g)	Activity (counts)	Counting time (sec)	Annealing time (sec)	Thermal expansion $\Delta L/L$	Specimen diameter (inch)
						$\times 10^4$		
1099	T28-6	12.65807	12.62985	4086	850	6.480	0.00920	0.5501
	-7	12.76653	12.72622	4369	930			
	-8	12.82194	12.78944	4192	1500			
	-9	12.84409	12.80721	2072	1000			
	-10	12.86929	12.83788	3199	2500			
Background				686	1450			
1154	T29-1	12.48619	12.44833	4358	290	4.32	0.00976	0.5500
	-2	12.50830	12.46940	4209	330			
	-3	12.69168	12.65938	4073	420			
	-4	12.72993	12.69298	4096	420			
	-5	12.80188	12.76619	4087	540			
	-6	12.87970	12.84297	4083	660			
	-7	12.89040	12.86045	4071	1050			
	-8	13.07934	13.04552	4352	1330			
	-9	13.09295	13.05274	2418	1000			
	-10	13.09924	13.06182	1979	1200			
Background				636	1500			
1200	T30-1	12.46680	12.44834	4173	500	2.61	0.01024	0.5500
	-2	12.50187	12.46944	4678	350			
	-3	12.68984	12.65939	4034	350			
	-4	12.73054	12.69299	4410	350			
	-5	12.80184	12.76622	4367	450			
	-6	12.87729	12.84298	4282	550			
	-7	12.89748	12.86047	4197	650			
	-8	13.06562	13.04563	4067	1400			

TABLE IV (continued)

Annealing temperature (°C)	Section number[a]	Gross weight (g)	Tare weight (g)	Activity (counts)	Counting time (sec)	Annealing time (sec)	Thermal expansion $\Delta L/L$	Specimen diameter (inch)
						$\times 10^4$		
1200	T30-9	13.09279	13.05782	4082	1100	2.61	0.01024	0.5500
	-10	13.09717	13.06190	3104	1200			
	-11	13.10233	13.06872	1737	1000			
	-12	13.12872	13.09184	1328	1030			
	-13	13.14285	13.10290	978	1000			
Background				5041	10,920			
1250	T31-1	11.92177	11.90130	5940	750	1.68	0.01074	0.5496
	-2	12.55123	12.51806	4257	300			
	-3	12.57669	12.53900	4485	300			
	-4	12.61534	12.58117	3738	300			
	-5	12.65082	12.61673	4416	400			
	-6	12.66637	12.62990	4369	450			
	-7	12.75839	12.72624	3982	550			
	-8	12.82781	12.78947	4116	660			
	-9	12.84329	12.80723	4013	900			
	-10	12.87755	12.83788	4134	1200			
	-11	13.27092	13.23932	4085	2000			
	-12	13.29275	13.25331	3964	2300			
	-13	13.36692	13.33274	1331	1200			
	-14	13.41738	13.38724	1605	1850			
	-15	13.44541	13.40745	1734	2400			
Background				1260	2600			
1308	T32-1	12.46884	12.44835	4096	320	0.996	0.01124	0.5498
	-2	12.50141	12.46945	4206	270			
	-3	12.69331	12.65941	4219	290			
	-4	12.70942	12.69301	17,662	2840			

TABLE IV (continued)

Annealing temperature (°C)	Section number[a]	Gross weight (g)	Tare weight (g)	Activity (counts)	Counting time (sec)	Annealing time (sec)	Thermal expansion $\Delta L/L$	Specimen diameter (inch)
						$\times 10^4$		
1308	T32-5	12.80312	12.76621	4604	350		0.01124	0.5498
	-6	13.10256	13.06874	4095	390			
	-7	13.12747	13.09187	4053	460			
	-8	13.13969	13.10290	4076	580			
	-9	13.15391	13.11969	4084	790			
	-10	13.24588	13.20855	4033	960			
	-11	12.87578	12.84301	2873	1060			
	-12	12.89505	12.86047	2205	1040			
	-13	13.08199	13.04562	1587	1010			
	-14	13.09723	13.05780	5716	4750			
Background				1379	2910			
1370	T33-1	11.93093	12.90127	4025	380	0.786	0.01196	0.5497
	-2	12.55429	12.51801	4051	310			
	-3	12.57570	12.53897	4138	320			
	-4	12.61615	12.58114	4216	380			
	-5	12.65304	12.61670	4070	410			
	-6	12.66418	12.62985	4037	500			
	-7	12.75865	12.72621	4001	610			
	-8	12.82463	12.78942	4010	700			
	-9	12.84393	12.80718	4748	1000			
	-10	12.87088	12.83785	3261	1010			
Background				1379	2910			
1450	T35-1	12.47084	12.44834	4768	580	0.510	0.01278	0.5499
	-2	12.50405	12.46944	4075	360			
	-3	12.69525	12.65940	4087	350			
	-4	12.72533	12.69300	4225	440			

TABLE IV (continued)

Annealing temperature (°C)	Section number[a]	Gross weight (g)	Tare weight (g)	Activity (counts)	Counting time (sec)	Annealing time (sec)	Thermal expansion $\Delta L/L$	Specimen diameter (inch)
						$\times 10^4$		
1450	T35-5	12.79919	12.76619	4075	450		0.01278	0.5499
	-6	12.87829	12.84300	4004	470			
	-7	12.89313	12.86047	4558	650			
	-8	13.08567	13.04555	4409	600			
	-9	13.08875	13.05772	4447	920			
	-10	13.09621	13.06180	4907	1110			
	-11	13.10449	13.06865	4061	1060			
	-12	13.12459	13.09176	2954	1070			
	-13	13.14142	13.10280	5398	2130			
	-14	13.15318	13.11961	5178	3060			
	-15	13.24704	13.20846	5219	3350			
Background				1017	2180			
1500	T36-1	11.91747	11.90128	4085	700	0.390	0.01328	0.5498
	-2	12.55364	12.51803	4141	350			
	-3	12.56841	12.53897	5930	570			
	-4	12.61606	12.58114	5181	470			
	-5	12.65087	12.61668	4306	450			
	-6	12.66327	12.62985	4348	500			
	-7	12.75864	12.72621	4077	520			
	-8	12.82404	12.78943	4032	560			
	-9	12.84140	12.80720	4071	630			
	-10	12.87885	12.83785	4549	810			
	-11	13.26342	13.23920	3413	1010			
	-12	13.28885	13.25318	3411	850			
	-13	13.36616	13.33263	10,182	3310			

TABLE IV (continued)

Annealing temperature (°C)	Section number[a]	Gross weight (g)	Tare weight (g)	Activity (counts)	Counting time (sec)	Annealing time (sec)	Thermal expansion $\Delta L/L$	Specimen diameter (inch)
						$\times 10^4$		
1500	T36-14	13.41826	13.38214	2285	870		0.01328	0.5498
	-15	13.44134	13.40736	2502	1250			
Background				930	2030			
1543	T37-1	12.47741	12.44834	5856	760	0.270	0.01372	0.5500
	-2	12.49981	12.46944	4105	530			
	-3	12.69613	12.65939	4095	440			
	-4	12.72529	12.69298	4049	540			
	-5	12.80050	12.76621	4174	550			
	-6	12.87472	12.84299	4053	660			
	-7	12.89293	12.86047	4534	780			
	-8	13.08588	13.04562	4055	640			
	-9	13.09068	13.05780	8526	1950			
	-10	13.09900	13.06187	3948	1000			
	-11	13.10380	13.06872	8821	2770			
	-12	13.12960	13.09183	2771	1000			
	-13	13.13389	13.10288	1973	1000			
	-14	13.15775	13.11968	1794	1050			
	-15	13.24360	13.20851	1386	1000			
Background				776	1700			

[a]Specimens T5 through T20 are for the diffusion of titanium-44 and specimens T24 through T37 are for the diffusion of vanadium-48.

The experimental data necessary for the calculation of a diffusion coefficient are: the section thicknesses or some parameter from which the thicknesses may be calculated, the specific activity of each section, and the time of the diffusion anneal. In this experiment, the individual section weights, density, specimen diameter, and the linear thermal expansion were used to calculate the section thicknesses. The specific activities were calculated from the activity at a constant x-ray energy level, the time to register this activity, and the weight of the section. Sample T20 (Appendix C, page 57) in which titanium-44 was diffused will be used to illustrate such a calculation.

The weight of the first section is the difference between the gross and tare weights for Sample T20-1, page 57 :

$$\begin{array}{r} 12.48400 \text{ grams} \\ -\underline{12.44835} \\ 0.03565 \text{ gram.} \end{array}$$

Similarly, the weight of each section is calculated.

The weight of a section divided by the bulk density and the area of the specimen yields the section thickness. This calculation must be made assuming the specimen is at the annealing temperature. For the first section of Sample T20, page 57, the thickness is

$$x = \frac{\text{weight}}{\dfrac{\text{density}}{\left(\dfrac{L+\Delta L}{L}\right)^3} \times \text{area} \times \left(\dfrac{L+\Delta L}{L}\right)^2} = \frac{\text{weight} \times L+\Delta L/L}{\text{density} \times \text{area}}$$

$$x = \frac{0.03565 \text{ g} \times 1.01023 \text{ cm/cm}}{4.53 \text{ g/cm}^3 \times \pi/4 \times (0.5495 \text{ in.} \times 2.54 \text{ cm/in.})^2}$$

$$x = 2.667 \times 10^{-3} \text{ cm.}$$

The penetration distance squared as plotted on the abscissa in Figures 6 and 7 (pages 25 and 26) is calculated as follows. The activity of each section is taken to be at the midpoint of the section so that the penetration distance, x_n, of the nth section is the total thickness of sections starting at zero and including the $(n - 1)$ section plus one half the thickness of the nth section.

The specific activity of a section is

$$A = \frac{\dfrac{\text{activity}}{\text{counting time}} - \text{background}}{\text{section weight}}$$

For the section of Sample T20-1, page 53 ,

$$A = \frac{\dfrac{4421 \text{ counts}}{509 \text{ sec}} - \dfrac{1204 \text{ counts}}{2460 \text{ sec}}}{35.65 \text{ mg}} = 0.2299 \text{ counts/sec mg} .$$

The logarithm of the specific activity is plotted on the ordinate in Figures 6 and 7 (pages 25 and 26).

The slope of the plot of ln $A(x,t)$ versus x^2 is $-1/4Dt$ where t is the annealing time or, from Figure 6, page 25, the 1200°C plot:

$$D = \frac{x_2^2 - x_1^2}{4t \ln \dfrac{A_1}{A_2}} = \frac{(207.6 \times 10^{-5} - 0) \text{ cm}^2}{(4 \times 2.358 \times 10^4 \times \ln 10) \text{ sec}}$$

$$D = 9.56 \times 10^{-9} \text{ cm}^2/\text{sec} .$$

APPENDIX D

```
      PROGRAMDIFFUSE
      DIMENSIONA(30),X(30),C(30),AA(6),TITLE(4),Z(30),Y(30),CT(30)
      COMMONA,X,C,NCY,ITOPY,XMAX,DELX,AINT,AFIN,D,DEV,Z,Y,CT
   91 READINPUTTAPE10,1,TEMP
    1 FORMAT(F10.0)
      IF(TEMP)90,90,2
    2 READINPUTTAPE10,10,BKGR,TIME,XLINEX,DIAM,RHO,TAU,J,JI,JK
   10 FORMAT(6F10.0,3I3)
      READINPUTTAPE 10,110,(A(I),CT(I),X(I),Z(I),I=1,J)
  110 FORMAT(4F10.0)
      CALLCALC(BKGR,J,JK,JI,TIME,XLINEX,RHO,DIAM,TAU)
      CALLSEMLOG(NCY,ITOPY,0.,DELX,10,15,,-7,AA)
      CALLCURVE(1,0.,AINT,AA)
      CALLCURVE(2,XMAX,AFIN,AA)
      DO70I=1,J
   70 CALLPOINT(I,Y(I),A(I),4,0,08,0.,1,AA)
      CALLLETTER(1,15,15HX *10     (CM ) ,AA)
      CALLEXPON(1,15,1,1H2,AA)
      CALLEXPON(1,15,5,1H5,AA)
      CALLEXPON(1,15,12,1H2,AA)
      CALLLETTER(2,29,29HSPECIFIC  ACTIVITY   (C,P,S,),AA)
      CALLHOLLER(29,TITLE,10)
      CALLLETTER(0,29,TITLE,AA)
      CALLSYMBOL(9,5,9,5,,21,2HD=,0,,2)
      CALLNUMBER(10.0,9,5,0,21,D,0,,5HE11,4)
      CALLSYMBOL(12,0,9,5,0,21,12H(CM**2/SEC,),0.,12)
      CALLSYMBOL(9,5,9,0,0,21,20H90 PCT. CONF,=+ OR -,0.,20)
      CALLNUMBER(13,3,9,0,0,21,DEV,0,,5HE11,4)
      CALLADVANCE(AA)
      GOTO91
   90 CALLEXIT
      END DIFFUSE
      SUBROUTINECALC(B,J,JK,JI,T,XL,R,G,TAU)
      DIMENSIONA(30),X(30),C(30),Z(30),Y(30),CT(30)
      COMMONA,X,C,NCY,ITOPY,XMAX,DELX,AINT,AFIN,D,DEV,Z,Y,CT
      K=0
      SUMX=0.
      SUMA=0.
      SUMASQ=0.
      SUMAX=0.
      SUMXSQ=0.
      C(1)=X(1)*0.5
      DO 40 M=2,J
   40 C(M)=C(M-1)+0.5*(X(M-1)+X(M))
      DO50I=1,J
      IF(I-JK)55,55,51
   51 K=1
   55 Y(I)=((C(I)*XL)/(250.*R*(G*2.54)**2*3.14159))**2
       A(I)=A(I)/CT(I)
      C(I)=LOGF(A(I))
```

```
      IF(TAU)58,58,59
   59 C(I)=C(I)+LOGF(2.0)*Z(I)/TAU
      A(I)=EXPF(C(I))
   58 A(I)=(A(I)-B)/X(I)
      C(I)=LOGF(A(I))
      IF(K)50,57,50
   57 IF(I-JI)50,50,90
   90 L=I
      SUMX=SUMX+Y(I)
      SUMA=SUMA+C(I)
      SUMASQ=SUMASQ+C(I)**2
      SUMAX=SUMAX+C(I)*Y(I)
      SUMXSQ=SUMXSQ+Y(I)**2
   50 CONTINUE
      AB=L-JI
      XMAX=Y(L)
      BINX=SUMXSQ-SUMX**2/AB
      BINAX=SUMAX-SUMA*SUMX/AB
      BINA=SUMASQ-SUMA**2/AB
      SLOPE=BINAX/BINX
      AINT=(SUMA-SLOPE*SUMX)/AB
      SUMDSQ=BINA-BINAX**2/BINX
      SQRT=SQRTF((AB-2.)*BINX/SUMDSQ)
      CALLSTUDENT(L,TEST)
      DEV=TEST/SQRT
      AFIN=AINT+XMAX*SLOPE
      D=-0.25/(SLOPE*T)
      DEV=-0.25/((SLOPE+DEV)*T)-D
      IF(AINT-C(1))30,30,31
   30 NAINT=C(1)*.434294
      GOTO32
   31 NAINT=AINT*.434294
   32 IF(AFIN-C(J))33,33,34
   33 NC=AFIN*.434294
      GOTO35
   34 NC=C(J)*.434294
   35  NCY=NAINT-NC+2
      ITOPY=NAINT+1
      AINT=EXPF(AINT)
      AFIN=EXPF(AFIN)
      DO60I=1,J
   60 Y(I)=Y(I)*10.**5
      XMAX=XMAX*10.**5
      DO12I=1,7
      AI=I
      AI=10.**(AI-5.)
      DO12L=2,10,2
      AL=L
      YMAX=AI*AL
       IF(Y(J)-YMAX)5,12,12
   12 CONTINUE
    5 DELX=YMAX/10.
      RETURN
```

```
      END
      SUBROUTINESTUDENT(L,TEST)
      GOTO(1,2,3,4,5,6,7,8,9,10,11,12,13,14,15,16,17,18,19,20,
     121,22,23,24,25,26,27,28,29,30)L
    1 TEST=6.314
      RETURN
    2 TEST=2.920
      RETURN
    3 TEST=2.353
      RETURN
    4 TEST=2.132
      RETURN
    5 TEST=2.015
      RETURN
    6 TEST=1.943
      RETURN
    7 TEST=1.895
      RETURN
    8 TEST=1.860
      RETURN
    9 TEST=1.833
      RETURN
   10 TEST=1.812
      RETURN
   11 TEST=1.796
      RETURN
   12 TEST=1.782
      RETURN
   13 TEST=1.771
      RETURN
   14 TEST=1.761
      RETURN
   15 TEST=1.753
      RETURN
   16 TEST=1.746
      RETURN
   17 TEST=1.740
      RETURN
   18 TEST=1.734
      RETURN
   19 TEST=1.729
      RETURN
   20 TEST=1.725
      RETURN
   21 TEST=1.721
      RETURN
   22 TEST=1.717
      RETURN
   23 TEST=1.714
      RETURN
   24 TEST=1.711
      RETURN
   25 TEST=1.708
```

```
      RETURN
   26 TEST=1.706
      RETURN
   27 TEST=1.703
      RETURN
   28 TEST=1.701
      RETURN
   29 TEST=1.699
      RETURN
   30 TEST=1.697
      RETURN
      END
         FINIS
```

ORNL-3616
UC-25 — Metals, Ceramics, and Materials
TID-4500 (29th ed.)

INTERNAL DISTRIBUTION

1–3. Central Research Library
4. Reactor Division Library
5–6. ORNL — Y-12 Technical Library Document Reference Section
7–26. Laboratory Records Department
27. Laboratory Records, ORNL RC
28. ORNL Patent Office
29. W. K. Bierman
30. C. M. Blood
31. T. F. Connolly
32. J. L. Cook
33. F. L. Culler
34. J. E. Cunningham
35. J. I. Federer
36. J. H Frye, Jr.
37. D. Heitkamp
38–42. M. R. Hill
43. D. O. Hobson
44. H. W. Joy
45. G. W. Keilholtz
46. R. F. Lafferty, Jr.
47. C. E. Larson
48. T. S. Lundy
49. H. G. MacPherson
50–74. J. F. Murdock
75. J. J. Pinajian
76. R. E. Reed
77. J. O. Stiegler
78. J. A. Swartout
79. M. S. Wechsler
80. J. R. Weir
81. W. J. Werner
82. R. P. Wichner
83. A. M. Weinberg
84. F. R. Winslow
85. A. A. Burr (consultant)
86. J. R. Johnson (consultant)
87. C. S. Smith (consultant)
88. R. Smoluckowski (consultant)

EXTERNAL DISTRIBUTION

89. C. M. Adams, Jr., Massachusetts Institute of Technology
90. D. E. Baker, General Electric, Hanford
91–92. D. F. Cope, AEC, ORO
93. Ersel Evans, General Electric, Hanford
94. J. L. Gregg, Cornell University
95. Research and Development, AEC, ORO
96. J. Simmons, AEC, Washington, D.C.
97. L. M. Slifkin, University of North Carolina
98. E. E. Stansbury, University of Tennessee
99. D. K. Stevens, AEC, Washington, D.C.
100–598. Given distribution as shown in TID-4500 (29th ed.) under Metals, Ceramics, and Materials category.